Journal of Pharmaceutical and Biomedical Analysis 222 (2023) 115036

Contents lists available at ScienceDirect

Journal of Pharmaceutical and Biomedical Analysis

journal homepage: www.journals.elsevier.com/journal-of-pharmaceutical-and-biomedical-analysis

Electrochemistry of chemotherapeutic alkylating agents and their interaction with DNA

Ana-Maria Chiorcea-Paquim [a,b,*,1], Ana Maria Oliveira-Brett [a,b,*,2]

[a] Department of Chemistry, Centre for Mechanical Engineering, Materials and Processes – CEMMPRE, University of Coimbra, 3004-535 Coimbra, Portugal
[b] Instituto Pedro Nunes, 3030-199 Coimbra, Portugal

ARTICLE INFO

Keywords:
Alkylating agents
Electrochemistry
DNA-drugs interaction
DNA-electrochemical biosensor
Oxidative DNA damage

ABSTRACT

Alkylating agents were among the first anticancer drugs to be discovered and continue to be the most commonly used in chemotherapy. They are electrophiles that react with the ring nitrogen and extracyclic oxygen atoms of DNA bases, forming covalent adducts that further lead to cross-linking of DNA strands, abnormal base pairing or DNA strand breaks. The investigation and quantitative analysis of alkylating agents in biological samples are essential for monitoring the therapy progression and efficiency, understanding their pharmacokinetics and develop new more effective and specific chemotherapeutical drugs. Among biotechnological methods, electrochemical techniques are particularly important in pharmaceutical medicine, owing to their rapid detection, great sensitivity, robustness, exceptional detection limits, ability to be used with small analyte volumes in turbid biofluids, and easy adaptability to miniaturization and point-of-care (POC) testing. This article provides first an exhaustive review concerning the electrochemical methods of characterization and quantification of different classes of chemotherapeutic alkylating agents (triazenes and hydrazines, nitrosoureas, nitrogen mustards, oxazaphosphorines, alkyl alkane sulfonates and ethylene imines) in standard samples, pharmaceutical formulations and biological matrixes. The second part of the article focuses on the recent electrochemical methodologies and DNA-electrochemical biosensors developed to study the interaction of alkylating agents with DNA. These studies are relevant for obtaining real-time details about the alkylating agents' mechanism of action and for assessing the oxidative DNA damage they cause, important for the development of improved antineoplastic drugs.

1. Introduction

Alkylating agents were among the first anticancer drugs to be discovered, after observing their effects during their use as chemical weapons during the First World War. Nowadays they are still the most commonly used pharmacological compounds in chemotherapy.

Alkylating agents are electrophiles that react with the nucleophilic moieties of DNA, resulting in the covalent transfer of an alkyl group. In the alkylation reaction (1) [1,2], a nucleophilic substitution occurs, in which the hydrogen H atom of the nucleophilic target of alkylation (H-R') is substituted by the alkyl group R of the alkylating agent (R-X, with X being a negatively charged halogen atom, e.g. chlorine).

$$\text{R-X} + \text{H-R'} \rightarrow \text{R-R'} + \text{HX} \quad (1)$$

Alkylating agents react directly with the ring nitrogen N and extracyclic oxygen O atoms of DNA bases, Fig. 1, to form covalent adducts that can vary from simple methyl groups to complex alkyl additions that can further cause cross-linking of DNA strands, abnormal base pairing or DNA strand breaks [3].

The type of DNA lesions caused by an alkylating agent depends on its number of reactive sites (monofunctional or bifunctional alkylating agent), its chemical reactivity (S_N1 or S_N2 type nucleophilic substitution), the type of alkyl group addition (methyl, chloroethyl, etc.) and DNA type (double-stranded or single-stranded) [3]. Monofunctional alkylating agents contain one active chemical moiety, interacting with only one DNA strand and generating covalent adducts, whereas bifunctional alkylating agents contain two reactive groups, interacting with two atoms on both DNA strands and generating intra-strand cross-links. S_N2 alkylating agents target ring N atoms, whereas S_N1 alkylating agents target both ring N and extracyclic O atoms in DNA bases, Fig. 1b.

* Correspondence to: Department of Chemistry, Faculty of Sciences and Technology, University of Coimbra, 3004-535 Coimbra, Portugal.
E-mail addresses: anachior@ipn.pt (A.-M. Chiorcea-Paquim), brett@ci.uc.pt (A.M. Oliveira-Brett).
[1] https://orcid.org/0000-0002-0605-5147.
[2] https://orcid.org/0000-0002-6244-0891.

https://doi.org/10.1016/j.jpba.2022.115036
Received 7 June 2022; Received in revised form 6 September 2022; Accepted 7 September 2022
Available online 9 September 2022

There are five traditional classes of chemotherapeutic alkylating agents, Table 1: triazenes and hydrazines (e.g. temozolomide, dacarbazine, procarbazine), nitrosoureas (e.g. streptozotocin, carmustine, lomustine, nimustine, fotemustine), nitrogen mustards (e.g. mechlorethamine, bendamustine, chlorambucil, melphalan, estramustine), oxazaphosphorines (e.g. cyclophosphamide, ifosfamide), alkyl alkane sulfonates (e.g. busulfan), and ethylene imines or aziridines (e.g. altretamine, thiotepa, mitomycin C) [1,3,4].

Over the last years, new alkylating agents, especially nitrogen mustard hybrid compounds, have been synthetized [5]. However, the alkylating agent's effectiveness in slow-growing cancers, but not on rapidly growing ones, their lack of site specificity, which leads to side effects on normal non-tumor cells, and the ability of the body to acquire chemoresistance, which leads to treatment failure, are important drawbacks in alkylating agents-based cancer therapy. Therefore, the development of new more effective and specific chemotherapeutical alkylating agents is of outmost importance. The quantitative pharmaceutical analysis of alkylating agents in biological samples is also important for understanding their pharmacokinetics and monitoring the therapy progression. Electrochemical techniques received increased attention in biotechnological applications in pharmacology, due to their rapid detection, great sensitivity, robustness, easy miniaturization, excellent detection limits, use of small analyte volumes, ability to be used in turbid biofluids and adaptability to the point-of-care (POC) testing.

The design and applications of electrochemical techniques of characterization and quantitative determination of different classes of chemotherapeutic alkylating agents (nitrogen mustards, oxazaphosphorines, alkyl alkane sulfonates, ethylene imines, nitrosoureas and triazenes and hydrazines) in standard samples, pharmaceutical

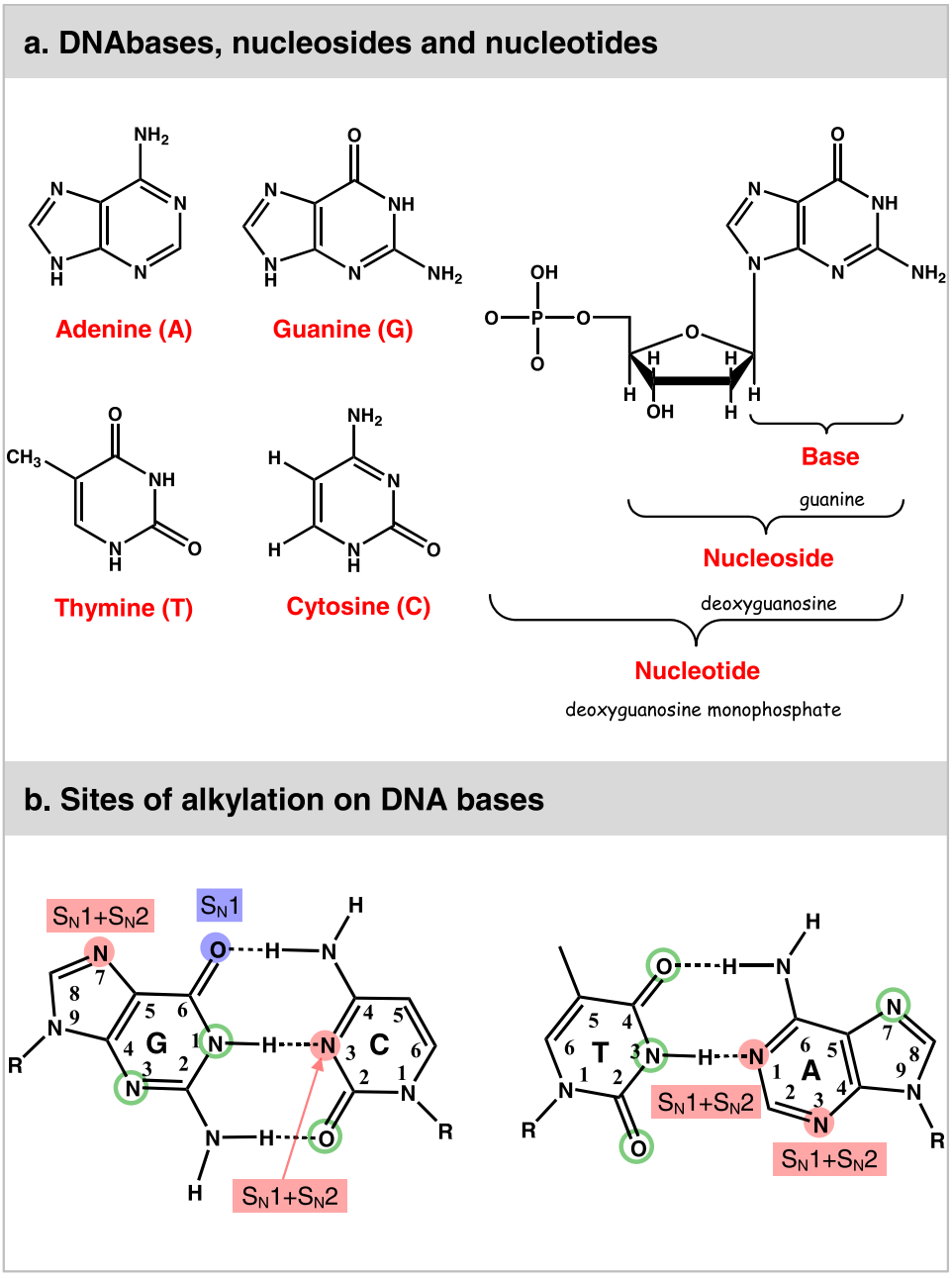

Fig. 1. (a) Chemical structures of DNA bases, nucleosides and nucleotides, (b) Sites of alkylation on DNA bases, with the major sites shown in red and blue, and with the minor sites shown in green.

Table 1
The main classes of alkylating agents used in clinic treatment.

Class of alkylating agents	Drugs	Clinical use
MONOFUNCTIONAL		
Triazenes and hydrazines		
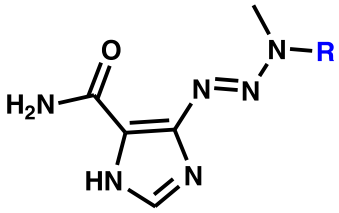	Temozolomide	Glioblastoma multiforme, anaplastic astrocytoma
	Dacarbazine	Melanoma, Hodgkin's lymphoma
	Procarbazine	Stage III and stage IV Hodgkin's lymphoma
Nitrosoureas		
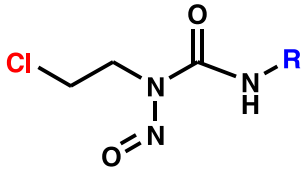	Streptozotocin	Metastatic pancreatic islet cell carcinoma
	Carmustine	Brain tumours, multiple myeloma
	Lomustine	Brain tumors, Hodgkin's lymphoma
	Nimustine	Glioblastoma
BIFUNCTIONAL		
Nitrogen mustards		
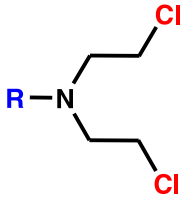	Mechlorethamine	Hodgkin disease, chronic leukemias, lung cancer
	Bendamustine	Chronic lymphocytic leukemia, non-Hodgkin lymphoma
	Chlorambucil	Chronic lymphocytic leukemia, Hodgkin's and non-Hodgkin's lymphomas
	Melphalan	Multiple myeloma, ovarian cancer
	Estramustine	Prostate cancers
Oxazaphosphorines		
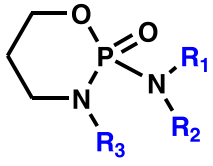	Cyclophosphamide	Lymphomas, myelomas, leukemia, neuroblastoma, ovarian adenocarcinoma, retinoblastoma, breast carcinoma
	Ifosfamide	Testicular, ovarian, cervical, bladder, lung cancers, osteocarcinoma, non-Hodgkin's lymphoma
Alkyl alkane sulfonates		
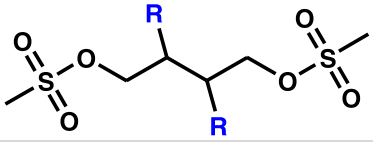	Busulfan	Chronic myelogenous leukemia
Ethylene imines		
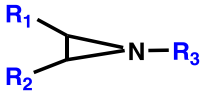	Altretamine	Ovarian cancer
	Thiotepa	Adenocarcinoma, bladder carcinomas
	Mitomycin C	Lip, oral, pharynx, digestive, peritoneum, breast and bladder cancers

compounds and biological matrixes, are described, Table 2. Recent advances in the electrochemical characterization methodologies, and DNA-electrochemical biosensor applications for studying the interaction of alkylating agents with DNA, are presented. The details about the alkylating agents' real-time mechanism of action, and the oxidative DNA damage they cause, were discussed.

2. Electrochemical sensing of alkylating agents

2.1. Triazenes and hydrazines

Triazenes present three adjacent N atoms, their main representatives being the monofunctional agents temozolomide (also known Temodal) and dacarbazine (also known as deticene or DTIC), Fig. 2. Both compounds are prodrugs that undergo spontaneous chemical degradation at physiologic pH to form the highly unstable 5-(3-methyltriazen-1-yl) imidazole-4-carboxamide (MTIC), that is further hydrolyzed to 5-amino-imidazole-4-carboxamide (AIC) and methyldiazonium ion [3,6], Fig. 3a, considered responsible for the alkylation of the DNA bases, Fig. 3b. Temozolomide is capable of crossing the blood-brain barrier, therefore being recommended for the treatment of glioblastoma multiforme and refractory anaplastic astrocytoma, while dacarbazine is recommended for metastatic malignant melanoma, Hodgkin's disease, soft tissue sarcomas, neuroblastoma, fibrosarcomas, rhabdomyosarcoma, islet cell carcinoma, and medullary carcinoma of the thyroid.

Temozolomide electrochemical behavior at glassy carbon electrode (GCE) was studied [6], showing that its reduction is an irreversible pH-dependent process that involves the addition of one electron and one proton at the C5 position, forming an anion radical and causing the irreversible break of the tetrazinone ring. The temozolomide oxidation is an irreversible and adsorption-controlled process for pH < 5.2, occurring in two steps and leading to the formation of a hydroxylated product, Fig. 4. The electroanalytical determination of temozolomide at GCE was achieved [6], showing a linear range from 2.0×10^{-6} to 1.3×10^{-5} M, a limit of detection (LOD) of 1.1×10^{-6} M and a limit of quantification (LOQ) of 3.7×10^{-6} M.

The temozolomide chemical degradation in aqueous solutions to its major metabolite AIC, Fig. 3a, was investigated at GCE, following the pH-dependent changes in the temozolomide electrochemistry behavior, i.e. the increase of the anodic peak current and disappearance of the cathodic peak [7]. AIC oxidation revealed to be irreversible, diffusion-controlled and pH-dependent up to a pH close to the pKa, occurring in two steps that lead to the formation of two reversible redox products. A mechanism for AIC oxidation was proposed.

The electroanalytical determination of temozolomide was achieved at a sensor based on a nanocomposite formed by reduced graphene oxide (rGO) silver nanocube (AgNC) hybrid decorated molecularly imprinted polymer (MIP), immobilized onto a screen-printed carbon electrode (SPCE) [8]. The rGO/AgNC@MIP-SPCE sensor showed: (i) in standard solutions, a linear range from 1.1×10^{-7} to 1.4×10^{-7} g/mL and a LOD of 1.6×10^{-10} g/mL, (ii) in blood plasma, a linear range from 1.2×10^{-7} to 1.4×10^{-7} g/mL and a LOD of 2.4×10^{-10} g/mL, (iii) in pharmaceutical formulations, a linear range from 1.3×10^{-7} to 1.4×10^{-7} g/mL and a LOD of 3.1×10^{-10} g/mL, and (iv) in urine samples, a linear range 1.1×10^{-7} to 1.3×10^{-7} g/mL and a LOD of 4.2×10^{-10} g/mL.

The redox behavior of dacarbazine and of its metabolite AIC at carbon paste electrode (CPE) was studied by linear sweep voltammetry (LSV) and differential pulse voltammetry (DPV) [9]. The oxidation of both dacarbazine and AIC occurred in two steps, each with the transfer of two electrons, yielding the same final product, the 5-hydroxyimidazol-4-carboxamide.

The dacarbazine redox behavior was studied by Tast polarography and differential pulse polarography (DPP) at dropping mercury electrode (DME), by cyclic voltammetry (CV) and DPV at hanging mercury drop electrode (HMDE), and by anodic voltammetry at GCE [10]. Calibration graphs were achieved: (i) at HMDE by DPP, in the linear range from 2.0×10^{-8} to 2.0×10^{-5} M, with a LOD of 4.0×10^{-9} M, (ii) at HMDE by adsorptive stripping voltammetry, in the linear range from 5.0×10^{-9} to 1.0×10^{-5} M, and (iii) at GCE by high-performance liquid chromatography (HPLC) with amperometric detection, from 1.0×10^{-5} to 1.0×10^{-4} M. The methods were compared, showing that the determination of dacarbazine at HMDE by DPP is the most efficient, and evaluated for the dacarbazine determination in blood serum.

Dacarbazine interacts with Cu(II) ions, forming a 1:1 complex. The electrochemical reduction of the dacarbazine–Cu(II) complex was investigated at HMDE, being associated with the irreversible one-electron reduction of the Cu(II) ions directly within the complex [11]. Based on the dacarbazine–Cu(II) complex adsorption and interfacial accumulation, the dacarbazine electroanalytical determination was achieved, showing: (i) in bulk form, a linear range from 4.0×10^{-10} to 2.1×10^{-8} M, a LOD of 2.7×10^{-10} M and a LOQ of 9.2×10^{-10} M, (ii) in vial, a linear range from 1.9×10^{-9} to 3.6×10^{-8} M, a LOD of 6.1×10^{-10} M and a LOQ of 2.0×10^{-9} M, (iii) in human urine, a linear range from 5.0×10^{-10} to 1.2×10^{-8} M, a LOD of 1.6×10^{-10} M and a LOQ of 5.2×10^{-10} M, and (iv) in human serum, a linear range from 1.9×10^{-9} to 5.7×10^{-8} M, a LOD of 2.0×10^{-9} M and a LOQ of 6.6×10^{-9} M [11].

Dacarbazine electrochemical behavior was studied on a sodium dodecyl sulfate (SDS) modified CPE (SDS/CPE), and its oxidation mechanism was proposed [12]. The results showed that dacarbazine oxidation is irreversible and diffusion controlled, involving the transfer of two protons and two electrons. The dacarbazine electroanalytical determination was achieved: (i) by CV in the linear range from 1.0×10^{-5} to 7.0×10^{-5} M, with a LOD of 8.2×10^{-7} M and a LOQ of 1.0×10^{-5} M, and (ii) by DPV in the linear range from 1.0×10^{-6} to 4.0×10^{-6} M, with a LOD of 1.5×10^{-7} M and a LOQ of 1.0×10^{-5} M [12]. In a different report, a sensor based on multiwall carbon nanotube (MWCNT) modified CPE was developed [13], that allowed the dacarbazine quantification in the linear range from 4.0×10^{-10} to 4.0×10^{-8} M and from 4.0×10^{-8} to 2.5×10^{-6} M, with a LOD of 1.2×10^{-10} M and a LOQ of 4.0×10^{-10} M. The proposed sensor showed high sensitivity, stability and percentage of recovery in pharmaceutical samples.

A tin doped ceria nanoparticles (NPs) modified glassy carbon paste electrode (GCPE) for the dacarbazine determination was developed [14]. The dacarbazine was selectively detected in the presence of other electroactive species and metal ions. The Sn–CeO_2NPs/GCPE sensor showed by square wave voltammetry (SWV): (i) in standard solutions, a linear range from 6.4×10^{-8} to 6.7×10^{-6} M and a LOD of 3.8×10^{-9} M, (ii) in serum samples, a linear range from 7.6×10^{-8} to 6.6×10^{-6} M and a LOD of 6.0×10^{-9} M, and (iii) in urine samples, a range from 6.9×10^{-8} to 5.3×10^{-6} M and a LOD of 6.3×10^{-9} M [14].

An electrochemical sensor based on MWCN paste electrode (CNPE) and poly(2-amino-1,3,4-thiadiazole) (poly-ATD) conducting polymer also was developed [15]. The dacarbazine electroanalytical quantification at the poly-ATD/CNPE sensor was achieved by DPV, with a linear range from 5.0×10^{-8} to 2.4×10^{-5} M and a LOD of 3.5×10^{-8} M. The sensor was tested in artificial urine and pharmaceutical formulations.

In a different report, a sensor based on MIP nanospheres (NSPs) modified pencil graphite electrode (PGE) was also achieved [16]. For the electrochemical detection of dacarbazine, the MIP-NSPs/PGE sensor showed: (i) in standard solutions, a linear range from 1.0×10^{-10} to 5.1×10^{-8} g/mL and a LOD of 2.0×10^{-11} g/mL, (ii) in blood plasma, a linear range from 1.0×10^{-10} to 4.5×10^{-8} g/mL and a LOD of 2.0×10^{-11} g/mL, (iii) in pharmaceutical formulations, a linear range from 1.0×10^{-10} to 4.8×10^{-8} g/mL and a LOD of 3.0×10^{-11} g/mL, and (iv) in urine samples, a linear range 1.2×10^{-10} to 4.8×10^{-8} g/mL and a LOD of 3.0×10^{-11} g/mL.

Procarbazine, Fig. 2, belongs to the hydrazines family, being a monofunctional alkylating agent used in the therapy of Hodgkin's disease and malignant melanoma. Procarbazine is also a prodrug that generates the highly reactive diazonium ion.

Table 2
Selected studies concerning the electroanalytical determination of alkylating agents.

Alkylating agents	Sensor/biosensor	Sample type	Linear range	LOD	LOQ	Ref.
MONOFUNCTIONAL						
Triazenes and hydrazines						
Temozolomide	GCE	standard	2.0×10^{-6}–1.3×10^{-5} M	1.10×10^{-6} M	3.7×10^{-6} M	[6]
	rGO/AgNC@MIP-SPCE	standard	1.1×10^{-7}–1.4×10^{-7} g/mL	1.6×10^{-10} g/mL	—	[8]
		in blood plasma	1.2×10^{-7}–1.4×10^{-7} g/mL	2.4×10^{-10} g/mL		
		pharmaceutical	1.3×10^{-7}–1.4×10^{-7} g/mL	3.1×10^{-10} g/mL		
		urine	1.1×10^{-7}–1.3×10^{-7} g/mL	4.2×10^{-10} g/mL		
Dacarbazine	HMDE	standard	2.0×10^{-8}–2.0×10^{-5} M	4.0×10^{-9} M	—	[10]
	HMDE	bulk	4.0×10^{-10}–2.1×10^{-8} M	2.7×10^{-10} M	9.2×10^{-10} M	[11]
		vial	1.9×10^{-9}–3.6×10^{-8} M	6.1×10^{-10} M	2.0×10^{-9} M	
		urine	5.0×10^{-10}–1.2×10^{-8} M	1.6×10^{-10} M	5.2×10^{-10} M	
		serum	1.9×10^{-9}–5.7×10^{-8} M	2.0×10^{-9} M	6.6×10^{-9} M	
	SDS/CPE	standard	1.0×10^{-6}–4.0×10^{-6} M	1.5×10^{-7} M	1.0×10^{-5} M	[12]
	MWCNT/CPE	standard	4.0×10^{-10}–4.0×10^{-8} M 4.0×10^{-8}–2.5×10^{-6} M	1.2×10^{-10} M	4.0×10^{-10} M	[13]
	Sn–CeO_2NPs/GCPE	standard	6.4×10^{-8}–6.7×10^{-6} M	3.8×10^{-9} M	—	[14]
		serum	7.6×10^{-8}–6.6×10^{-6} M	6.0×10^{-9} M		
		urine	6.9×10^{-8}–5.3×10^{-6} M	6.3×10^{-9} M		
	poly-ATD/CNPE	standard	5.0×10^{-8}–2.4×10^{-5} M	3.5×10^{-8} M		[15]
	MIP-NSPs/PGE	standard	1.0×10^{-10}–5.1×10^{-8} g/mL	2.0×10^{-11} g/mL	—	[16]
		plasma	1.0×10^{-10}–4.5×10^{-8} g/mL	2.0×10^{-11} g/mL		
		pharmaceutical	1.0×10^{-10}–4.8×10^{-8} g/mL	3.0×10^{-11} g/mL		
		urine	1.2×10^{-10}–4.8×10^{-8} g/mL	3.0×10^{-11} g/mL		
	dsDNA/SPCE	standard	—	2.0×10^{-8} M	5.9×10^{-8} M	[82]
	dsDNA/SWCNT/PGE	standard	2.0×10^{-6}–1.0×10^{-5} M	1.1×10^{-6} M	—	[84]
Nitrosoureas						
Streptozotocin	Polyaniline/GCE	standard	3.0×10^{-6}–5.0×10^{-6} M	1.25×10^{-10} M	2.35×10^{-8} M	[21]
	HMDE	standard	1.0×10^{-7}–1.0×10^{-3} M	2.5×10^{-8} M	7.4×10^{-8} M	[22]
	HMDE	standard	2.0×10^{-7}–1.0×10^{-4} M	7.0×10^{-8} M	2.4×10^{-7} M	[25]
Carmustine	GCE	standard	6.5×10^{-6}–1.1×10^{-3} M	4.2×10^{-7} M	1.4×10^{-6} M	[24]
	HMDE	standard	2.0×10^{-7}–1.0×10^{-4} M	1.9×10^{-7} M	6.2×10^{-7} M	[25]
	m-AgSAE	standard	2.0×10^{-6}–1.0×10^{-4} M	2.1×10^{-7} M	7.1×10^{-7} M	[25]
	m-AgSAE in FIA	standard	6.0×10^{-6}–1.0×10^{-4} M	2.2×10^{-7} M	7.1×10^{-7} M	[25]
Lomustine	m-AgSAE	standard	2.0×10^{-6}–1.0×10^{-4} M	6.6×10^{-7} M	2.2×10^{-6} M	[25]
	AgSAE	standard	1.0×10^{-6}–1.0×10^{-4} M	1.5×10^{-7} M	4.9×10^{-7} M	[26]
	MF/PGE	bulk	1.9×10^{-7}–1.4×10^{-5} M	8.1×10^{-8} M	2.7×10^{-7} M	[27]
		urine	3.8×10^{-7}–2.4×10^{-5} M	3.0×10^{-7} M	1.0×10^{-6} M	
		serum	1.9×10^{-6}–2.8×10^{-5} M	3.9×10^{-7} M	1.3×10^{-6} M	
Nimustine	nimustine-TPB/CPE	standard	1.0×10^{-5}–1.0×10^{-2} M	4.8×10^{-6} M	—	[28]
	nimustine-TPB/β-CD/CPE	standard	1.0×10^{-7}–1.0×10^{-2} M	5.0×10^{-8} M		
	nimustine-TPB/CNT/CPE	standard	1.0×10^{-8}–1.0×10^{-2} M	7.9×10^{-9} M		

(*continued on next page*)

Table 2 (*continued*)

Alkylating agents	Sensor/biosensor	Sample type	Linear range	LOD	LOQ	Ref.
BIFUNCTIONAL						
Nitrogen mustards						
Bendamustine	PGE	standard	5.0×10^{-6}–8.0×10^{-5} g/mL	6.0×10^{-6} g/mL	2.0×10^{-5} g/mL	[29]
Chlorambucil	MnO_2@$NiFe_2O_4$ NP/GCE	standard	2.5×10^{-5}–5.7×10^{-4} M	4.7×10^{-6} M	—	[31]
	C60-monoadduct-micellar MIP/IL-CCE	standard	1.5×10^{-9}–2.5×10^{-7} g/mL	3.6×10^{-10} g/mL	—	[32]
		plasma	1.6×10^{-9}–2.4×10^{-7} g/mL	3.9×10^{-10} g/mL		
		urine	1.6×10^{-9}–2.4×10^{-7} g/mL	5.1×10^{-10} g/mL		
		pharmaceutical	1.6×10^{-9}–2.4×10^{-7} g/mL	3.9×10^{-10} g/mL		
	PVCL/PPy semi-IPN MGs/GCE	standard	2.0×10^{-8}–4.2×10^{-4} M	2.0×10^{-9} M	—	[33]
	dsDNA/PPy/FLPt/$NiCo_2O_4$/PGE	standard	1.8×10^{-8}–2.0×10^{-4} M	4.0×10^{-9} M	—	[92]
Melphalan	GCE	standard	1.0×10^{-3}–1.0×10^{-6} M	1.0×10^{-6} M	—	[34]
	DME	standard	2.0×10^{-5}–1.0×10^{-3} M	—	8.0×10^{-6} M	[35]
Oxazaphosphorines						
Cyclophosphamide	GCE	standard	5.0×10^{-5}–1.75×10^{-4} M	1.1×10^{-6} M	3.7×10^{-6} M	[36]
	N,S-AGR/MIP/GE	standard	8.0×10^{-12}–8.0×10^{-7} M	3.4×10^{-12} M	—	[37]
Ifosfamide	Ti_3C_2/MWCNT/Chit/GCE	standard	1.1×10^{-9}–1.0×10^{-6} M	3.1×10^{-10} M	—	[40]
	Au/Pd@rGO@p(L-Cys)/PGE	standard	0.1×10^{-6}–9.0×10^{-5} M	9.2×10^{-9} M	—	[39]
		pharmaceutical		9.2×10^{-9} M		
		serum		9.3×10^{-9} M		
		urine		$9.\times10^{-9}$ M		
	Ti_3C_2/MWCNT/Chit/GCE	standard	1.1×10^{-9}–1.0×10^{-6} M	3.1×10^{-10} M	—	[40]
	GQDs-MIP/SPCE	standard	2.5×10^{-10}–1.2×10^{-6} g/mL	8.0×10^{-11} g/mL	—	[41]
		plasma	3.1×10^{-10}–1.2×10^{-6} g/mL	1.1×10^{-10} g/mL		
		urine	2.8×10^{-10}–1.1×10^{-6} g/mL	1.0×10^{-10} g/mL		
		pharmaceutical	3.2×10^{-10}–1.1×10^{-6} g/mL	1.0×10^{-6} g/mL		
Ethylene imines						
Mitomycin C	Fe_3O_4@$CuCo_2S_4$/GCE	standard	0.1×10^{-6}–2.0×10^{-5} M	8.0×10^{-10} M	—	[50]
	dsDNA/GO/PGE	standard	2.0×10^{-5} –1.2×10^{-4} g/mL	9.1×10^{-6} g/mL	—	[100]
	dsDNA/PoPDMWCNT/PGE	standard	5.0×10^{-7}–2.5×10^{-5} g/mL	1.2×10^{-8} g/mL	3.9×10^{-8} g/mL	[104]
	dsDNA/SWCNT-PVF^+/PGE	standard	—	6.25×10^{-7} g/mL	—	[105]

Abbreviations: AdsSV – adsorptive stripping voltammetry; AgNC – silver nanocube; AgSAE – silver solid amalgam electrode; CNPE – carbon nanotubes paste electrode; CPE – carbon paste electrode; CV – cyclic voltammetry; DME – dropping mercury electrode; DPASV – differential pulse anodic stripping voltammetry; DPCAdSV – differential pulse cathodic adsorptive stripping voltammetry; DPP – differential pulse polarography; DPV – differential pulse voltammetry; dsDNA – double-stranded DNA; FIA – flow injection analysis; FIA-ED – flow injection analysis with electrochemical detection; FLPt/NiCo2O4 – flower-like Pt/NiCo2O4 nanocomposites; GCE – glassy carbon electrode; GCPE – glassy carbon paste electrode; GO – graphene oxide; GQDs – graphene quantum dots; HMDE – hanging mercury drop electrode; IL-CCE – ionic liquid based carbon ceramic electrode; LOD – limit of detection; LOQ – limit of quantification; m-AgSAE – mercury meniscus modified silver solid amalgam electrode; MF – mercury film; MGs – microgels; MIP – molecularly imprinted polymer; MWCNT – multiwall carbon nanotube; N,S-AGR – nitrogen and sulfur co-doped activated graphene; NP – nanoparticle; p(L-Cys) – poly (L-Cysteine); PGE – pencil graphite electrode; poly-ATD – poly(2-amino-1,3,4-thiadiazole); PoPDMWCNT – poly(o-phenylenediamine); PPy – polypyrrole; PVCL – poly(N-vinylcaprolactam); PVF+ – poly(vinylferrocenium); rGO – reduced graphene oxide; SDS – sodium dodecyl sulfate; Sn–CeO2NPs – tin doped ceria nanoparticles; SPCE – screen printed carbon electrode; SWCASV – square wave cathodic adsorptive stripping voltammetry; SWV – square wave voltammetry; SWCNT – single wall carbon nanotube; TPB – sodium tetraphenylborate; TPB/CNT – carbon nanotube; β-CD – β-cyclodextrin.

Procarbazine redox behavior at GCE was investigated in the pH range from 3.3 to 11.2, using CV, DPV and SWV [17]. The results showed that procarbazine oxidation is irreversible and adsorption-controlled, occurring in four steps. The first, second and third steps are pH-dependent, occurring with the transfer of one electron and one proton and forming an electroactive product in acid media, whereas the forth oxidation step is pH-independent, occurring with the transfer of one electron. The proposed oxidation mechanism showed that the first and second oxidation steps occur at the hydrazine group, followed by isomerization, hydrolysis and formation of benzaldehyde procarbazine. The third and fourth oxidation steps occur at the benzaldehyde procarbazine with the formation of N-isopropylterephthalic acid [17]. Mathematical models of electrochemical oxidation of procarbazine in alkaline media [18] and in slightly alkaline on cobalt (III) oxyhydroxide medium [19] were investigated by means of linear stability theory and bifurcation analysis.

In another report, the procarbazine electrochemical reduction at mercury electrode showed four cathodic peaks [20]. The procarbazine oxidation in the presence of Ti(IV) was also investigated, showing that Ti(IV) coordination caused inhibition on its air oxidation, especially for oxidation catalyzed by Cu(II) ions [20].

2.2. Nitrosoureas

Streptozotocin (also known as streptozocin), Fig. 5, is a naturally occurring nitrosourea derived from *Streptomyces achromogenes*. This monufunctional alkylating agent is particularly toxic to the insulin-producing beta cells of the pancreas in mammals, being selectively transported into the pancreas cells by the glucose transport protein GLUT2, because of its structural similarity to glucose. Therefore, streptozotocin is used for the treatment of metastatic islet cell carcinoma of the pancreas and also to produce diabetes mellitus in medical research animals.

Streptozotocin electrochemical behavior at GCE modified with polyaniline was investigated [21], showing an irreversible reduction process in the pH range from 2.0 to 10.0, which occurs in two diffusion controlled steps. A possible electrochemical reduction mechanism was proposed. An electroanalytical method for the streptozotocin determination in the linear range from 3.0×10^{-6} to 5.0×10^{-6} M, with a LOD of 1.25×10^{-10} M and LOQ of 2.35×10^{-8} M, was developed and successfully applied for the streptozotocin determination in pharmaceutical and human urine samples.

Streptozotocin electrochemical reduction was investigated by direct current polarography, CV and DPP at a HMDE [22]. The streptozotocin direct quantitative determination, with a linear range from 1.0×10^{-7} to 1.0×10^{-3} M, a LOD of 7.4×10^{-8} M and a LOQ of 2.5×10^{-8} M, was achieved and applied in pharmaceutical formulation and spiked human urine samples, without interference from excipients. In another report, the carcinogenic potential of streptozotocin was evaluated by polarography [23].

Carmustine (BCNU), lomustine (CCNU) and nimustine (ACNU), Fig. 5, are synthetic nitrosurea monofunctional alkylating agents that have the ability to cross the blood-brain barrier, therefore being used to treat brain tumors (e.g. glioblastoma, brainstem glioma, medulloblastoma, astrocytoma, ependymoma and metastatic brain tumors), but also multiple myeloma, Hodgkin's disease, non-Hodgkin's lymphomas and cutaneous T-cell lymphoma.

Carmustine electrochemical behavior at GCE showed an irreversible, diffusion controlled and pH dependent reduction process, and a reduction mechanism was proposed [24]. The carmustine determination at GCE showed a linear range from 6.5×10^{-6} to 1.1×10^{-3} M, a LOD of 4.2×10^{-7} M and a LOQ of 1.4×10^{-6} M.

The voltammetric determination of streptozotocin, carmustine and lomustine was performed at HMDE and mercury meniscus modified silver solid amalgam electrode (AgSAE), m-AgSAE [25], showing better results by DPV: (i) streptozotocin at HMDE, a linear range from 2.0×10^{-7} to 1.0×10^{-4} M, a LOD of 7.0×10^{-8} M and a LOQ of 2.4×10^{-7} M, (ii) carmustine at HMDE, a linear range from 2.0×10^{-7} to 1.0×10^{-4} M, a LOD of 1.9×10^{-7} M and a LOQ of 6.2×10^{-7} M, (iii) carmustine at m-AgSAE, a linear range from 2.0×10^{-6} to 1.0×10^{-4} M, a LOD of 2.1×10^{-7} M and a LOQ of 7.1×10^{-7} M, and (iv) lomustine at m-AgSAE, a linear range from 2.0×10^{-6} to 1.0×10^{-4} M, a LOD of 6.6×10^{-7} M and a LOQ of 2.2×10^{-6} M. The methodology developed was applied for the determination of carmustine and lomustine in pharmaceutical formulations. Moreover, the m-AgSAE was employed for the carmustine determination by flow injection analysis (FIA), were, under optimized conditions, a linear range from 6.0×10^{-6} to 1.0×10^{-4} M, a LOD of 2.2×10^{-7} M and a LOQ of 7.1×10^{-7} M were achieved [25].

In another report, a methodology based on DPV with tubular detector in a flow system at a AgSAE was optimized for the electroanalytical detection of lomustine [26], showing a linear range from 1.0×10^{-6} to 1.0×10^{-4} M, a LOD of 1.5×10^{-7} M and a LOQ of 4.9×10^{-7} M. The method was successfully applied for the lomustine determination in real samples of the chemotherapy drug CeeNU Lomustine 40 mg.

An electrochemical sensor based on a mercury film (MF) coated PGE (MF/PGE) showed for the electroanalytical determination of lomustine

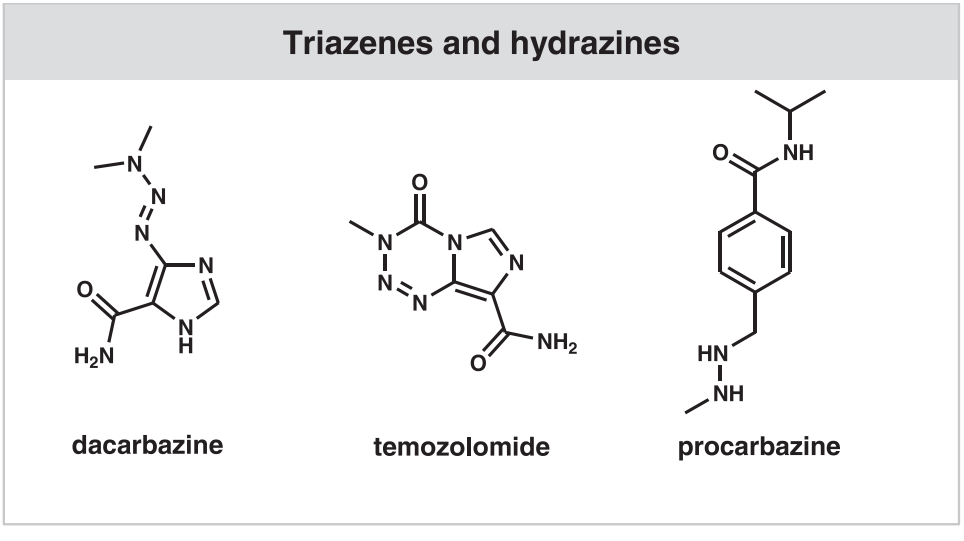

Fig. 2. Chemical structures of alkylating agents from triazenes and hydrazines class: dacarbazine, temozolomide and procarbazine.

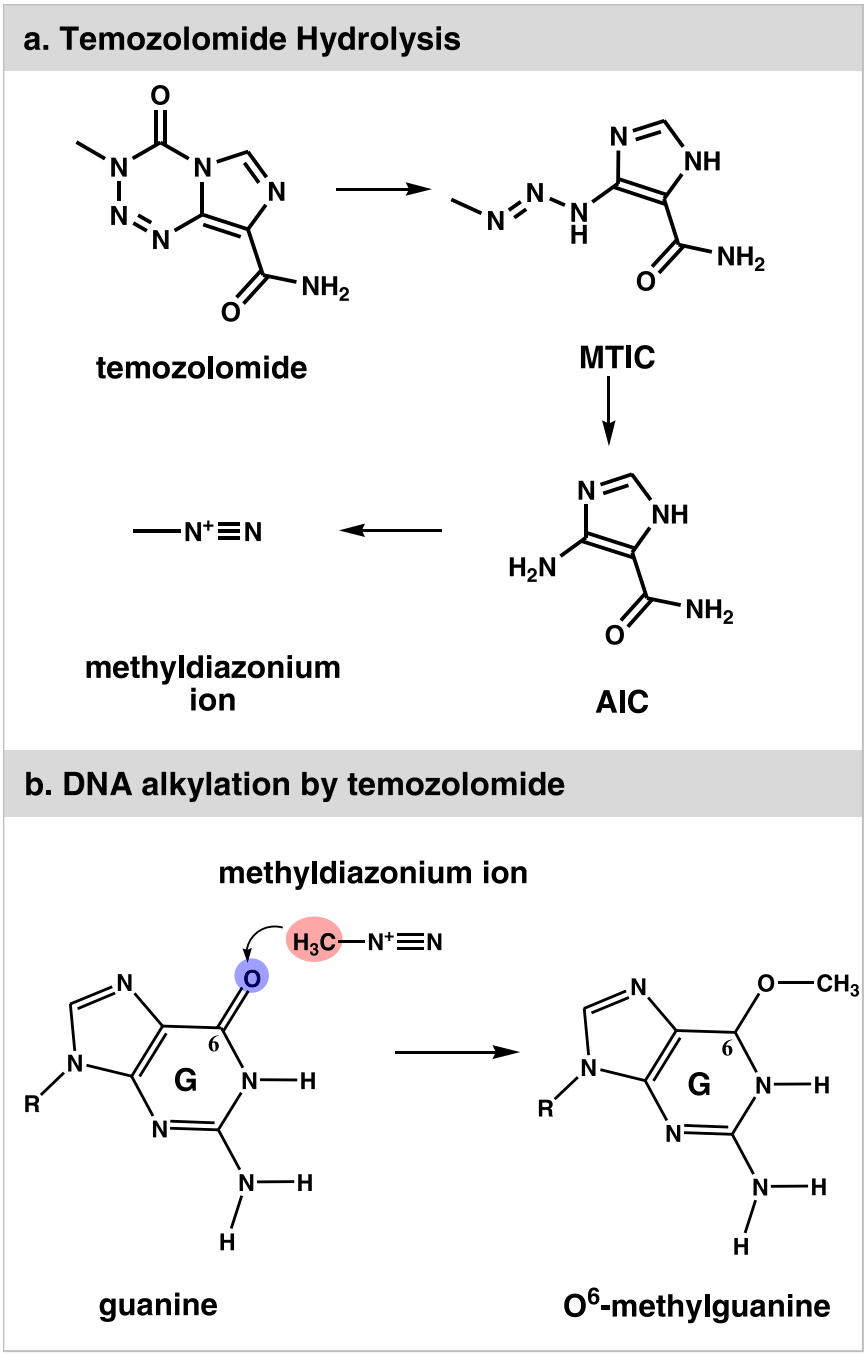

Fig. 3. (a) Hydrolysis of temozolomide to its metabolites, AIC and methyldiazonium ion, at physiological pH, (b) DNA alkylation reaction between temozolomide' metabolite methyldiazonium ion and guanine base at the O6 position, forming the O^6-methylguanine DNA lesion.

[27]: (i) in bulk, a linear range from 1.9×10^{-7} to 1.4×10^{-5} M, a LOD of 8.1×10^{-8} M and a LOQ of 2.7×10^{-7} M, (ii) in human urine, a linear range from 3.8×10^{-7} to 2.4×10^{-5} M, a LOD of 3.0×10^{-7} M and a LOQ of 1.0×10^{-6} M, and (iii) in human blood plasma, a the linear range from 1.9×10^{-6} to 2.8×10^{-5} M, a LOD of 3.9×10^{-7} M and a LOQ of 1.3×10^{-6} M.

The electroanalytical determination of nimustine was achieved at three CPE sensors [28]. For this purpose, the nimustine hydrochloride was incorporated with sodium tetraphenylborate (TPB) in the presence of orthonitrophenyloctyl ether as plasticizer, and then immobilized at the surface of bare CPE (the nimustine-TPB/CPE sensor), β-cyclodextrin (β-CD) modified CPE (the nimustine-TPB/β-CD/CPE sensor) and CNT-modified CPE (the nimustine-TPB/CNT/CPE sensor). The results showed (i) for nimustine-TPB/CPE sensor, a linear range from 1.0×10^{-5} to 1.0×10^{-2} M and a LOD of 4.8×10^{-6} M, (ii) for nimustine-TPB/β-CD/CPE sensor, a linear range from 1.0×10^{-7} to 1.0×10^{-2} M and a LOD of 5.0×10^{-8} M, and (ii) for nimustine-TPB/CNT/CPE sensor, a linear range from 1.0×10^{-8} to 1.0×10^{-2} M and a LOD of 7.9×10^{-9} M.

2.3. Nitrogen mustards

Nitrogen mustards, Table 1, are derivatives of sulfur mustards, being the first compounds used as chemotherapeutic agents for the treatment of leukemias and lymphomas.

Bendamustine, Fig. 6, is a bifunctional mechlor-ethamine derivative, recommended for the treatment of various lymphomas, multiple myeloma, lymphocytic leukemia, etc.

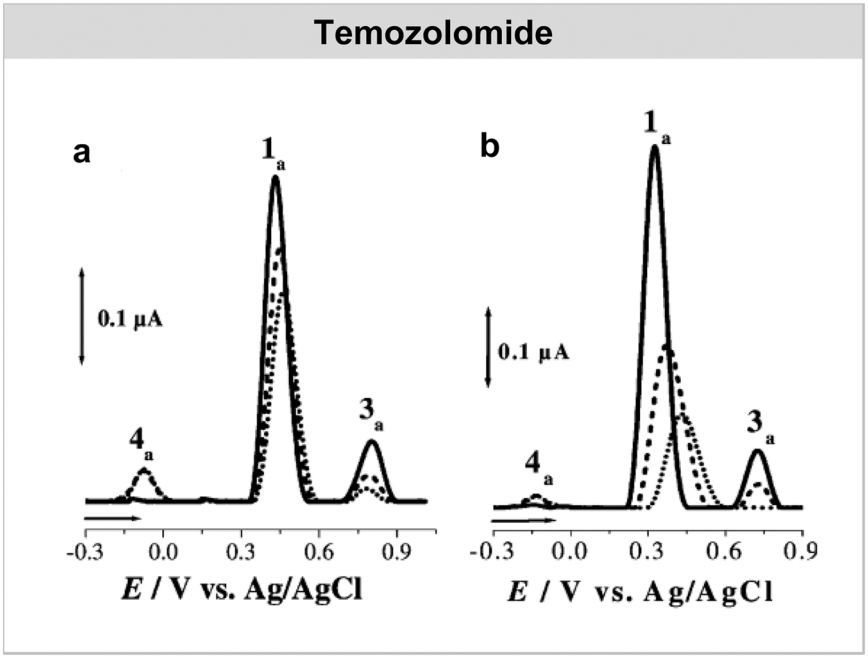

Fig. 4. DPVs baseline corrected of 500 µM temozolomide at GCE: (a) pH = 7.1, (b) pH = 9.1, (▬) first, (▬▬) second and (•••) third scans. Adapted from [6] with permission.

The bendamustine redox behavior was investigated at PGE, showing an irreversible, pH dependent, one-step oxidation, which occurs with the transfer of the same number of protons and electrons, and a one-step reduction. The bendamustine anodic peak was used for the electroanalytical determination of bendamustine in the linear range from 5×10^{-6} to 8.0×10^{-5} g/mL, with a LOD of 6.0×10^{-6} g/mL and a LOQ of 2.0×10^{-5} g/mL [29].

Chlorambucil, Fig. 6, is also a bifunctional alkylating agent that

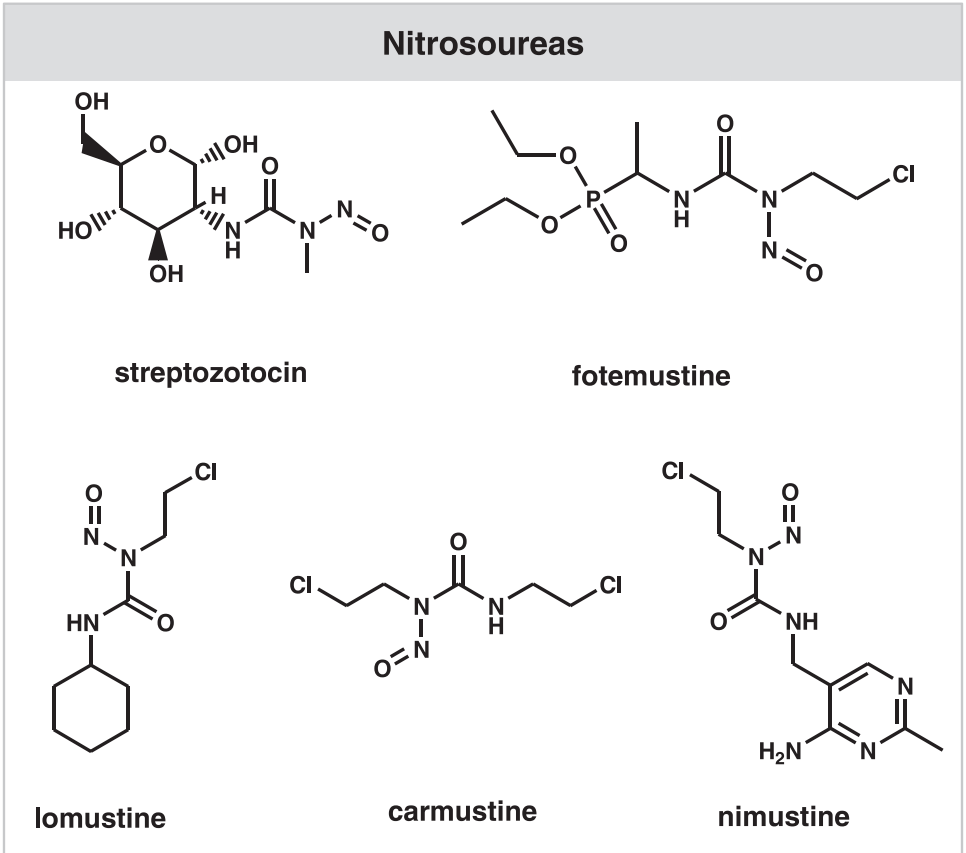

Fig. 5. Chemical structures of alkylating agents from nitrosoureas class: streptozotocin, fotemusine, lomustine, carmustine and nimusine.

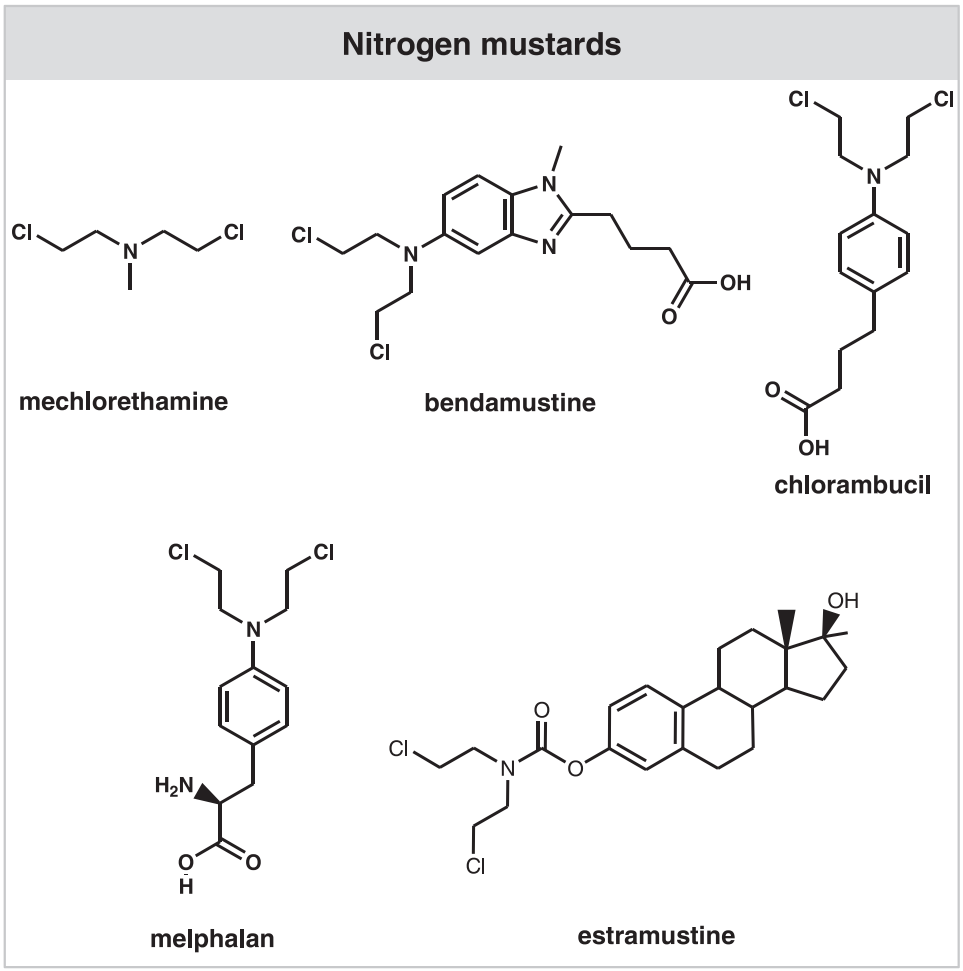

Fig. 6. Chemical structures of alkylating agents from nitrogen mustards class: mechlorethamine, bendamustine, chlorambucil, melphalan and estramustine.

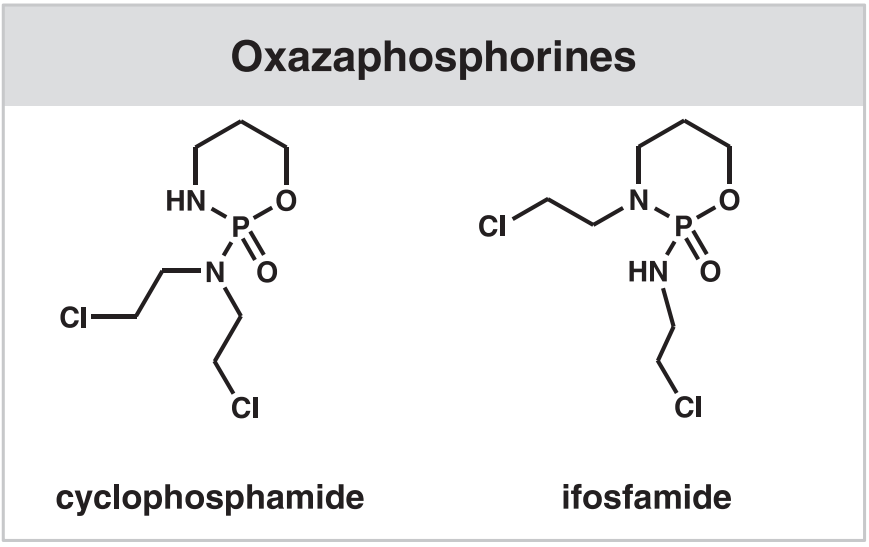

Fig. 7. Chemical structures of alkylating agents from oxazaphosphorines class: cyclophosphamide and ifosfamide.

forms cross-links with DNA. It is generally used to treat lymph node and blood cancers, including giant follicular lymphoma, leukemia, lymphosarcoma, chronic lymphocytic leukemia, lymphoma, Hodgkin's disease and rheumatoid arthritis.

Chlorambucil redox behavior was investigated at a platinum electrode in aqueous solution [30], showing one anodic and one cathodic peak that shifted to more negative potentials in the presence of 4-chloro butyronitrile.

Chlorambucil electroanalytical determination was achieved at a GCE modified by a MnO_2 @$NiFe_2O_4$ NPs nanocomposite [31]. The MnO_2 @$NiFe_2O_4$ NP/GCE sensor showed a linear range from 2.5×10^{-5} to 5.7×10^{-4} M and a LOD of 4.7×10^{-6} M, and presented a good selectivity in the presence of the interfering substances dopamine, uric acid, glucose, mercury, diphenylamine, sodium, potassium, nitrite, and diuron.

The electroanalytical determination of chlorambucil at a C60-monoadduct based micellar MIP at a ionic liquid based carbon ceramic electrode (IL-CCE), was also reported [32]. The C60-monoadduct-micellar MIP/IL-CCE sensor showed (i) in standard samples, a linear range from 1.5×10^{-9} to 2.5×10^{-7} g/mL and a LOD of 3.6×10^{-10} g/mL, (ii) in blood plasma, a linear range from 1.6×10^{-9} to 2.4×10^{-7} g/mL and a LOD of 3.9×10^{-10} g/mL, (iii) in urine, a linear range from 1.6×10^{-9} to 2.4×10^{-7} g/mL and a LOD of 5.1×10^{-10} g/mL, and (iv) in pharmaceutical formulations, a linear range from 1.6×10^{-9} to 2.4×10^{-7} g/mL and a LOD of 3.9×10^{-10} g/mL.

Chlorambucil was also electrochemically detected at a GCE modified by poly(N-vinylcaprolactam) semi-interpenetrated conductive polypyrrole microgels (PVCL/PPy semi-IPN MGs/GCE) [33], in the linear range from 2.0×10^{-8} to 4.2×10^{-4} M, with a LOD of 2.0×10^{-9} M, and tested in human blood serum and urine samples.

Melphalan, Fig. 6, is a phenylalanine derivative of nitrogen mustard that alkylates the DNA at the guanine N7 position, inducing DNA inter-strand cross-links. It is used for the treatment of multiple myeloma, ovarian cancer, neuroblastoma, rhabdomyosarcoma and breast cancer.

The melphalan anodic oxidation at GCE was investigated and the melphalan electroanalytical determination was achieved by DPV, showing a linear range from 1.0×10^{-3} to 1.0×10^{-6} M and a LOD of 1.0×10^{-6} M at both stationary and rotating (2000 rpm) GCEs [34]. The melphalan in ethanol-water medium (4:1) was also investigated by DPP at DME showing a linear range from 2.0×10^{-5} to 1.0×10^{-3} M and a LOQ of 8.0×10^{-6} M [35].

2.4. Oxazaphosphorines

Oxazaphosphorines (or oxazaphorines) are compounds based on nitrogen mustards, synthesized in order to improve their stability and reduce their toxicity. Cyclophosphamide (also known as cytophosphane among other names), Fig. 7, is a bifunctional nitrogen mustard activated in the liver by the cytochrome P450 microsomal system, to form the cytotoxic metabolites phosphoramide mustard and acrolein that can also cause DNA cross-links. Cyclophosphamide is used to treat cancer of the ovaries, breast, bone blood and lymph system. Ifosfamide, Fig. 7, is a bifunctional alkylating agent similar to cyclophosphamide, used in the treatment of lymphomas, sarcoma and advanced forms of solid organ cancer such as breast, testicular, ovarian, gastric and lung cancers.

The cyclophosphamide electrochemical behavior at CGE was investigated, showing one irreversible and diffusion controlled reduction peak [36]. The kinetic parameters were calculated and a reduction mechanism was proposed. The direct electroanalysis of cyclophosphamide at GCE, in the linear range from 5.0×10^{-5} to 1.75×10^{-4} M, with a LOD of 1.1×10^{-6} M and a LOQ of 3.7×10^{-6} M, was also achieved [36].

An electrochemical sensor based on nitrogen and sulfur co-doped activated graphene (N,S-AGR) and MIP at GCE showed, for the determination of cyclophosphamide, a linear range from 8.0×10^{-12} to 8.0×10^{-7} M and a LOD of 3.4×10^{-12} M [37]. In another report, the development of three poly(vinyl chloride) and poly(vinyl chloride) carboxylate membrane sensors for the determination of cyclophosphamide and ifosfamide was described [38].

Ifosfamide electroanalytical determination was also achieved at a PGE modified with Au/Pd@rGO nanocomposite and poly (L-Cysteine), in the presence of the antineoplastic chemotherapeutical drug etoposide [39]. The sensor showed a linear range from 1.0×10^{-7} to 9.0×10^{-5} M and a LOD of 9.2×10^{-9} M in standard solutions, 9.2×10^{-9} M in pharmaceutical formulation (injection solution), 9.3×10^{-9} M in serum and 9.3×10^{-9} M in urine samples.

A sensor based on GCE modified by MWCNT, Ti_3C_2 MXene and chitosan chit (Ti_3C_2/MWCNT/Chit composite) was developed [40], allowing the ifosfamide determination in the linear range from 1.1×10^{-9} to 1.0×10^{-6} M with a low LOD of 3.1×10^{-10} M. The sensor was successfully applied for the voltammetric screening of ifosfamide in urine and blood serum samples with recoveries higher than 95.21%.

An electrochemical sensor based on nanocomposites formed by graphene quantum dots (GQDs) and ifosfamide-selective MIPs, synthesized directly at the surface of SPCE (GQDs-MIP/SPCE) showed for the determination of ifosfamide [41]: (i) in standard samples, a linear range from 2.5×10^{-10} to 1.2×10^{-6} g/mL and a LOD of 8.0×10^{-11} g/mL, (ii) in blood plasma, a the linear range from 3.1×10^{-10} to 1.2×10^{-6} g/mL and a LOD of 1.1×10^{-10} g/mL, (iii) in urine, a the linear range from 2.8×10^{-10} to 1.1×10^{-6} g/mL and a LOD of 1.0×10^{-10} g/mL, and (iv) in pharmaceutical formulations, a the linear range from 3.2×10^{-10} to 1.1×10^{-6} g/mL and a LOD of 1.0×10^{-6} g/mL.

2.5. Alkyl alkane sulfonates

Among alkyl sulfonates, the bifunctional alkylating agent busulfan, Fig. 8, is the most representative antineoplastic drug. Busulfan is a bifunctional alkylating agent recommended for the treatment of chronic myeloid leukemia and certain blood diseases, such as polycythemia vera and myeloid metaplasia. In aqueous solution, busulfan undergoes hydrolysis to produce reactive carbonium ions that alkylate DNA. Although busulfan is widely used as chemotherapeutic agent, there is still lack of information concerning busulfan electrochemical behavior and its electroanalytical determination is not reported in the literature.

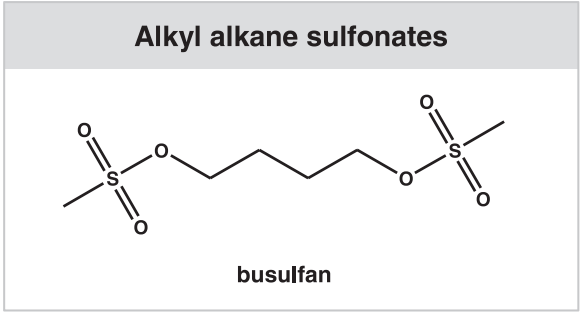

Fig. 8. Chemical structure of alkylating agent from alkyl alkane sulfonates class: busulfan.

2.6. Ethylene imines

Triethylenethiophosphoramide (also known as thiotepa or TT), Fig. 9, is a bifunctional alkylating agent belonging to the ethylene imines class, being used to treat ovarian, breast, and bladder cancers. Moreover, some thiotepa metabolites, such as tepa, monochlorotepa and thiotepa-mercapturate, also possess alkylating activity in vivo.

The electrochemical behavior of thiotepa at pH 4.2 [14,42] and of its hydrolysis product, thiotepa-SH [42], were investigated. The results showed that thiotepa reduction at mercury electrodes occurs in two steps, one diffusion and the other adsorption controlled [14].

Mitomycin C, Fig. 9, is a bifunctional alkylating acid with antibiotic properties, extracted from the fermentation of *Streptomyces* bacteria. Mitomycin C presents unique properties, due to the presence of two aziridine cycles and one quinone moiety. Clinically, mitomycin C is used to treat localized bladder, anal, head-and-neck and breast cancers.

DPP at HMDE, in the pH range from 5.0 to 10.0, showed that

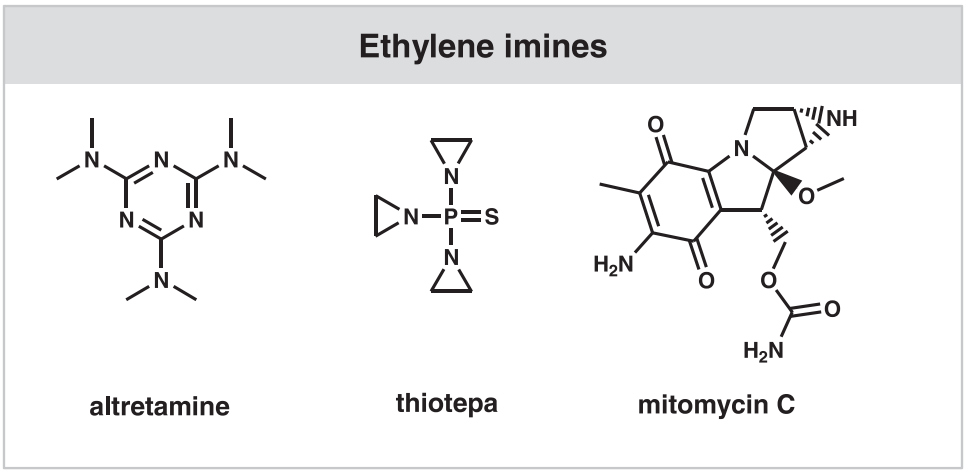

Fig. 9. Chemical structure of alkylating agents from ethylene imines class: altretamine, thiotepa and mitomycin C.

mitomycin C is present in two forms in equilibrium: a quinonoid form that undergoes a one-step reversible reduction to hydroquinone, that is further reduced in a two-step process, and a nonquinonoid form that that undergoes a one-step irreversible reduction at more negative potentials, the conversion of the nonquinonoid form into the quinone being acid catalyzed [43]. In another report, mitomycin C was investigated by polarography and CV in aqueous media, also showing its reversible reduction to the hydroquinone, followed by the aziridine ring opening [44]. The reduction mechanism was discussed in relation to the mitomycin C antineoplastic activity. The mitomycin C redox behavior was also studied at HMDE [45,46] and platinum electrode in dimethylformamide [47,48].

The mitomycin C oxidation behavior was investigated at CPE over a wide pH range [49]. The results showed a two-step diffusion-controlled irreversible oxidation process, one pH-independent for 2.2 < pH < 4.5 and the other one pH-dependent for 4.5 < pH < 12.0. The mitomycin C oxidation products are not electroactive at CPE. The mitomycin C spontaneous chemical degradation was electrochemically detected by the occurrence of a new oxidation peak at a lower potential. This chemical degradation product undergoes an irreversible, pH-dependent oxidation for 3.4 < pH < 5.4, its redox products being reversibly oxidized.

Mitomycin C electroanalytical determination was achieved in the presence of chemotherapeutic agent topotecan, using an electrochemical system, based on the Fe_3O_4 decorated on the surface of $CuCo_2S_4$ (Fe_3O_4 @$CuCo_2S_4$) nanocomposites at GCE [50]. The Fe_3O_4 @$CuCo_2S_4$/GCE sensor showed a linear range from 0.1×10^{-6} to 2.0×10^{-5} M and a LOD of 8.00×10^{-10} M.

3. Electrochemical sensing of alkylating agents interaction with DNA

3.1. Overview on electrochemistry of drugs interaction with DNA

Structure-based design strategies of pharmaceutical drugs, which take advantage of the drug interaction with specific DNA targets, have generated new DNA-binding agents with great clinical potential. Among various methods used to characterize the interaction of anticancer drugs with DNA molecules, electrochemical technics present the advantages of being fast, low cost, highly sensitive and selective, thus attracting considerable research efforts toward clinical diagnostics, drug development and biomedical applications.

DNA-electrochemical biosensors have received special attention, being able to detect changes of the DNA structure [51,52] and the occurrence of oxidative DNA damage [53–56]. According to IUPAC, an electrochemical DNA-electrochemical biosensor is a device consisting on an electrochemical transducer (the electrode) with a biological recognition element (the DNA film) immobilized on its surface [57]. DNA-electrochemical biosensor applications are generally based on detecting the interaction between the analyte under investigation and the immobilized DNA [58–64]. Using this approach, DNA-electrochemical biosensors have been successfully used to study DNA interactions with pharmaceutical drugs [63–68], proteins [51,69], hazard carcinogenic compounds, such as metal ions [70] pollutants [63], free radicals [71–73] and ionizing radiation [74], allowing the unraveling of detailed mechanistic interactions and to determine in real-time the DNA interaction mechanisms not only with the analyte, but also with its degradation and redox reaction products [75].

DNA-drug interactions are generally electrochemically studied measuring: (i) changes in the redox processes of the electroactive drug, (ii) changes in the redox behavior of the electroactive DNA base residues, usually the oxidation of G residues (G_r) and A residues (A_r) and (iii) occurrence of the oxidation signals of 8-oxoguanine (8-oxoG), 8-oxo-2′-deoxyguanosine (8-oxodG) and 2,8-dihydroxyadenine (2,8-DHA), biomarkers of oxidative DNA damage [55]. Thus, understanding the DNA electrochemical behavior at the surface of electrochemical transducer is essential.

The DNA bases, guanine (G), adenine (A), thymine (T) and cytosine (C), represent the electroactive moieties within DNA, and their oxidation at GCE follows the order: G ($E_p \sim +0.70$ V) < A ($E_p \sim +0.96$ V) < T ($E_p \sim +1.16$ V) < C ($E_p \sim +1.31$ V), vs. Ag/AgCl (3 M KCl), in pH = 7.4 [76], Fig. 10d. The 8-oxoG and 2,8-DHA ($E_p \sim +0.30$ V), vs. Ag/AgCl (3 M KCl), in pH = 7.4, biomarkers of oxidative DNA damage are more easily oxidized than G.

The oxidation of the DNA nucleosides, deoxyadenosine (dA), deoxyguanosine (dG), deoxythymidine (dT) and deoxycytidine (dC), occurs at the same potentials as the nucleotides, guanosine monophosphate (GMP), adenosine monophosphate (AMP), thymidine monophosphate (TMP) and cytidine monophosphate (CMP), following the same order, but shifted to more positive potentials when compared with the bases, since their bulkier structures difficult the electron transfer from the electroactive bases to the electrode surface: dG and GMP ($E_p \sim +0.95$ V) < dA and AMP ($E_p \sim +1.21$ V) < dT and TMP ($E_p \sim +1.41$ V) < dC and CMP ($E_p \sim +1.56$ V), vs. Ag/AgCl (3 M KCl), in pH = 7.4 [76], Fig. 10c.

The oxidation of double-stranded DNA (dsDNA) at GCE shows two small, pH-dependent anodic peaks, corresponding to the oxidation of G residues (G_r) and A residues (A_r) in the double-helical structure, Fig. 10a (▬) [60,62]. The T residues (T_r) and C residues (C_r) oxidation in the dsDNA present very low currents and occur at high positive potentials, near the potential of oxygen evolution, therefore they are not usually detected. The oxidation of ssDNA at GCE also corresponds to the G_r and A_r oxidation, Fig. 10a(▬), but the oxidation peak currents are greater

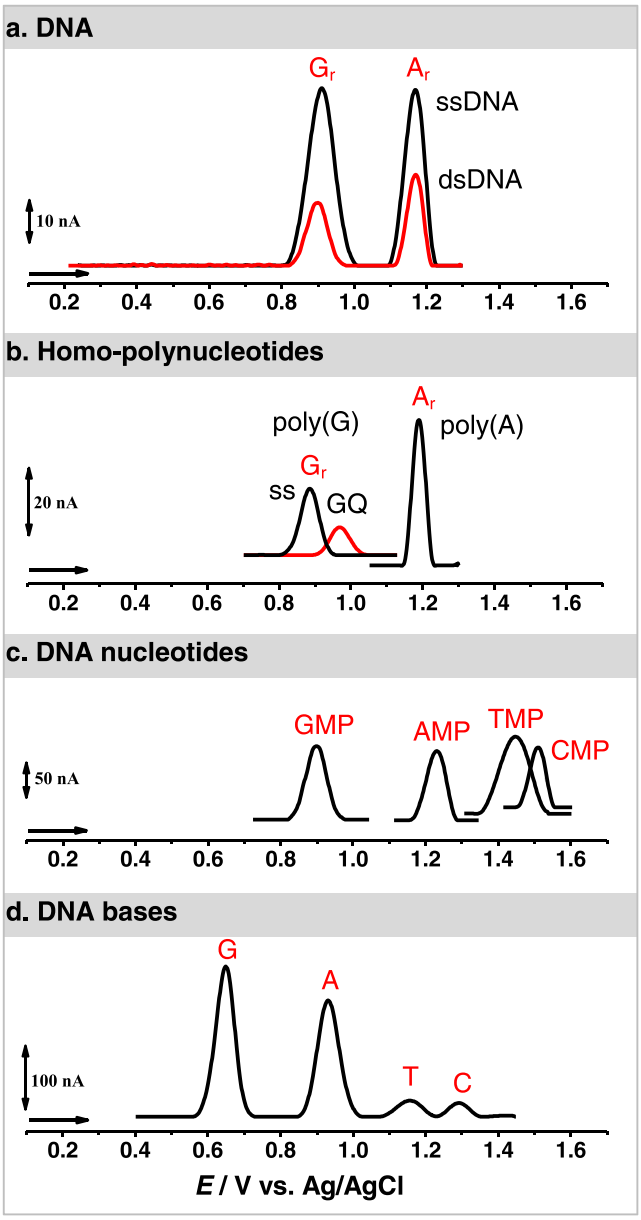

Fig. 10. DPVs baseline corrected at GCE, in solutions at pH 7.0: (a) 60 μg mL^{-1} dsDNA and 60 μg mL^{-1} ssDNA, (b) 5 μg mL^{-1} poly(G), 40 μg mL^{-1} poly(A), 100 μg mL^{-1} poly(T), 100 μg mL^{-1} poly(C), (c) 20 μM GMP, 20 μM AMP, 500 μM TMP, 500 μM CMP, and (d) 20 μM equimolar mixture of G, A, T and C. Adapted from [62,76] with permission.

than those of dsDNA, since the base residues in the ssDNA single-helix are in closer proximity to the electrode surface, thus presenting an easier electron transfer [77]. Therefore, the electrochemical methods are able to differentiate between different DNA secondary structures, and have been used to study the DNA structural modifications, such as transitions from/to single-, double-stranded and GQ secondary structures [51,52], Fig. 10a, b.

3.2. *Electrochemistry of alkylating agents interaction with DNA*

The interaction of temozolomide and its metabolites AIC and methyldiazonium ion with dsDNA was investigated by DPV at GCE, based on the changes of the G_r and A_r oxidation peak currents before and after interaction, Fig. 11 [78]. The results showed that temozolomide and AIC/methyldiazonium ion interact with dsDNA causing its condensation.

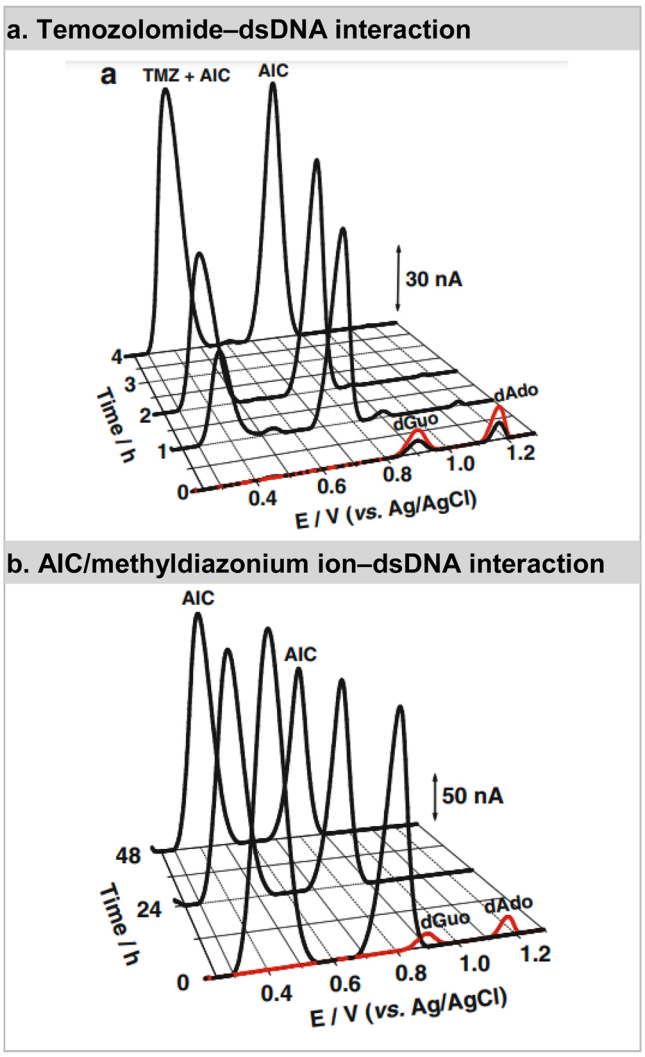

Fig. 11. DPVs baseline-corrected in pH 7.0 of 250 μg/mL dsDNA (▬) control and (▬) incubated with: (a) 250 μM temozolomide during 0, 1, 2 and 4 h and (b) 100 μM AIC/methyldiazonium ion during 0, 24 and 48 h.
Adapted from [78] with permission.

Studies concerning the temozolomide and AIC/methyldiazonium ion interaction with a multilayer dsDNA-electrochemical biosensor confirmed the dsDNA condensation and showed the occurrence of a new oxidation peak, corresponding to released free G bases from the DNA double-helix. This confirms that the temozolomide metabolites specifically interact with the G_r within DNA, causing its damage. Moreover, the occurrence of a new peak corresponding to the 8-oxoG/2,8-DHA oxidation confirms that oxidative DNA damage also occurs.

Using the same approach, the temozolomide interaction with dsDNA, single-stranded poly(A) and poly(G), and double-stranded poly(A)-poly(T) and poly(G)-poly(C) was studied at PGE [79]. The temozolomide-DNA interaction was also investigated at a DNA-electrochemical biosensor, based on the PGE modification by specific oligonucleotide sequences selected to contain the hypermethylation region of the Glutathione S-Transferase P-1 (GSTP-1), considered a promising biomarker of the prostate cancer [80]. The results showed that temozolomide causes localized distortion of the DNA, resulting in a wider major groove and greater steric accessibility.

A PGE modified with Au NPs and dsDNA (dsDNA/Au-NPs/PGE) electrochemical biosensor was developed and used for the electroanalytical determination of temozolomide in the linear range from 5.0×10^{-9} to 4.5×10^{-5} M, with a LOD of 1.0×10^{-9} M [81]. The

factors affecting the biosensor performance, such as the DNA concentration, interaction time and temperature, were optimized. Theoretical studies confirmed that the temozolomide intercalated into the dsDNA is stabilized by π-π interactions.

The interaction of dacarbazine with salmon sperm dsDNA was studied by CV and DPV at SPCE, and an analytical procedure for the dacarbazine determination at a dsDNA biosensor in spiked human serum samples was developed, showing a LOD of 2.0×10^{-8} M and a LOQ of 5.9×10^{-8} M [82].

The surface confined interaction between dacarbazine and dsDNA, ssDNA, poly(A), poly(G) and double stranded poly(A)-poly(T) and poly (G)-poly(C), immobilized at disposable PGE, was investigated by DPV and electrochemical impedance spectroscopy (EIS) [83]. Based on dacarbazine and G_r oxidation peaks, the dacarbazine interaction with fish sperm dsDNA was also investigated at disposable PGEs modified by single-walled carbon nanotubes (SWCN). This methodology allowed the detection of dacarbazine in the linear range from 2.0×10^{-6} to 1.0×10^{-5} M, with a LOD of 1.10×10^{-6} M [84].

The binding mode and the thermodynamic characteristics of dacarbazine and dacarbazine–Cu(II) complexes with calf-thymus dsDNA and ssDNA were also evaluated by CV, SWV and fluorescence spectroscopy [85]. The interaction of dacarbazine and dacarbazine–Cu(II) complexes with dsDNA occurs by intercalation into the base stacking domain, while the interaction with ssDNA is driven by electrostatic attractions. Based on the binding constants and thermodynamic parameters, a higher affinity towards DNA of the dacarbazine–Cu(II) complex, when compared with dacarbazine, was observed [85].

Studies concerning the dacarbazine binding to DNA or DNA bases in the presence of TiO_2 NPs showed that dacarbazine binding to purines G and A is stronger than to pyrimidines T and C, following the order of A > G > C > T, the TiO_2 NPs enhancing the detection sensitivity [86]. Similarly, a considerable enhancement of the binding affinity of dacarbazine to DNA and DNA bases was achieved in the presence of gold NPs [87,88].

In a different assay, dacarbazine was used as electrochemical probe to sensitively detect its sequence-specific binding and its ability to recognize a single A-G mismatch [89]. For this purpose, thiol-functionalized 15-mer oligonucleotides covalently attached on Au NPs and oligonucleotides covalently immobilized through chitosan onto GCE were employed. The results showed that dacarbazine binding affinity to purine bases is stronger than to pyrimidines.

The interaction of lomustine and its chemically degraded metabolites with dsDNA was investigated in solution and at a dsDNA-electrochemical biosensor [90]. The results showed that lomustine metabolites initially cause DNA condensation, followed by DNA unwinding. The release of free G bases and the occurrence of oxidative DNA damage were followed via the detection of the oxidation peaks of free G bases and 8-oxoG/2,8-DHA. Using poly(dA) and poly(dG) electrochemical biosensors, it was demonstrated that the lomustine metabolites cause oxidative DNA damage to both G_r and A_r.

A comparative study concerning the lomustine interaction with ssDNA e dsDNA at different temperatures and two pH values, pH = 7.4 of human blood and pH = 4.7 of stomach content [91], showed that lomustine intercalates efficiently between dsDNA bases at both pH values. The lomustine-ssDNA interaction was dependent on the ionic strength. The fact that the ionic shielding weakened the lomustine binding to ssDNA was consistent with a predominantly electrostatic interaction.

Bendamustine interaction with fish sperm dsDNA was investigated and the bendamustine toxicity degree was calculated, in the absence and presence of quercetin, a protective, natural flavonoid antioxidant shown to inhibit the bendamustine-DNA interaction [29]. Based on the chances of the G_r oxidation peak current before and after the DNA interaction with each compound, it was determined that bendamustine-DNA interaction decreases in the presence of quercetin, due to the quercetin competitive binding to DNA.

The chlorambucil interaction with a dsDNA-electrochemical biosensor, build by dsDNA immobilization onto a PGE modified with polypyrrole (Ppy) and flower-like Pt/NiCo2O4 nanocomposites (FLPt/$NiCo_2O_4$/PGE) was investigated [92]. Based on the G_r and A_r oxidation peak currents modifications, the chlorambucil electroanalytical determination, in the linear range from 1.8×10^{-8} and 2.0×10^{-4} M, with a LOD of 4.0×10^{-9} M, was achieved. The biosensor was then tested for chlorambucil determination in serum, urine and drug samples, showing recoveries of 97.5–103.8%.

The cyclophosphamide interaction with dsDNA and thermally denatured ssDNA immobilized at CPE and PGE was studied by DPV [93]. For the cyclophosphamide electrochemical detection, a DNA biosensor based on a CNT modified SPCE was also developed [94], the CNT modification leading to more uniform and stable DNA films, which result in faster response and a higher detection reproducibility.

The interaction of busulfan with salmon sperm dsDNA, in solution or immobilized onto SPCE, was investigated [95]. The busulfan-induced DNA damage was detected via the occurrence of the free G and A oxidation peaks. Moreover, crystal violet, which interacts with the DNA immobilized on SPCE, was used as an effective electroactive indicator, to monitor the cross-links or damage to DNA.

The thiotepa interaction with DNA was studied by voltammetric techniques and agarose gel electrophoresis. The results showed that the aziridine moiety is released from the thiotepa molecule and binds covalently to the N atoms of the DNA bases, leading to DNA strand breaks. The thiotepa interaction with calf thymus and supercoiled DNA was also investigated, showing important changes on the DNA peaks, consistent with the alkylation of the DNA bases in close proximity to the bases electroactive sites, the most probably major site of alkylation being the N7 position of purines, Fig. 1, which is strongly nucleophilic [14].

Mitomycin C was investigated by transfer stripping CV at a ssDNA-modified HMDE [96]. Acid and electroreductive mitomycin C activations were compared and different DNA-mitomycin C adducts were detected.

A multilayer dsDNA-electrochemical biosensor was used to evaluate the interaction between mitomycin C and DNA, showing that mitomycin C binds to the dsDNA immobilized onto a GCE surface, causing its condensation [49]. The oxidative DNA damage caused by mitomycin C metabolites was observed by the occurrence of the 8-oxoG/2,8-DHA oxidation peak. The interaction of mitomycin C with DNA was also investigated by voltammetry and EIS at CNTs modified PGE, SPCE and CPE, taking into consideration the G_r oxidation peak current modifications [97,98]. An electrochemical protocol for the direct monitoring of the mitomycin C–DNA interaction at a MWCNTs modified PGE was also described [99].

The interactions between surface-confined calf thymus dsDNA and mitomycin C were investigated using a graphene oxide (GO) modified PGE electrochemical sensor [100]. A signal enhancement of 21.4% and 34.4% of the oxidation peak currents of mitomycin C and G_r was achieved at the GO modified PGE, when compared with unmodified PGE. Based on the G_r oxidation peak current modifications, the electroanalytical determination of mitomycin C showed a linear range from 2.0×10^{-5} g/mL to 1.2×10^{-4} g/mL and a LOD of 9.1×10^{-6} g/mL. EIS studies revealed that the mitomycin C binding to dsDNA leads to a gradual decrease of its negative charge.

Biosensors based on MWCNT–chitosan modified PGE (CNTCHIT/PGE) [101] and a chitosan/ionic liquid modified PGE (CHIT-IL-PGEs) [102] were developed for enhanced electrochemical monitoring of calf thymus dsDNA interaction with mitomycin C. Both biosensors were evaluated and the experimental parameters were optimized.

A sensitive electrochemical biosensor based on a PGE modified with amino acid glycine or L-lysine nanoflowers was developed and evaluated for the detection of dsDNA, and of mitomycin C-dsDNA interactions [103]. The results showed that glycine nanoflowers-based sensors enhanced the sensor sensitivity in the detection of the G_r oxidation peak.

Mitomycin C electroanalytical detection was achieved at an electrochemical biosensor build via the dsDNA immobilization onto a poly (o-phenylenediamine)-MWCNT modified PGE (PoPDMWCNT/PGE) [104]. Measuring the G_r oxidation peak current modifications, the biosensor showed, for the mitomycin C detection, a linear concentration range from 5.0×10^{-7} to 2.5×10^{-5} g/mL, a LOD of 1.2×10^{-8} g/mL and a LOQ of 3.9×10^{-8} g/mL. The sensor was tested in serum samples [104]. In a different report, using a dsDNA SWCNT poly(vinylferrocenium) (PVF^{+}) modified PGE, a LOD of 6.25×10^{-7} g/mL was achieved [105].

Aiming to achieve a new drug-delivery system, mitomycin C was loaded into an oil/water system, and the interaction of the drug with the DNA in the microemulsion phase was investigated at PGE by DPV, via the variations of the G_r oxidation peak current [106].

4. Conclusions

Alkylating agents continue to be the most commonly used pharmacological compounds in chemotherapy, their mode of action being associated with the DNA damage that induces cell apoptosis. Due to their chemotherapeutic success, and aiming to overcome some of their drawbacks, the development of new more effective and specific chemotherapeutical alkylating agents is of outmost importance. The quantitative pharmaceutical analysis of alkylating agents in biological samples is also essential for understanding their pharmacokinetics and better monitoring the therapy progression.

This review presents a comprehensive overview concerning the design, development and applications of electrochemical methods, for the characterization and quantification chemotherapeutic alkylating agents belonging to the classes of triazenes and hydrazines, nitrosoureas, nitrogen mustards, oxazaphosphorines, alkyl alkane sulfonates and ethylene imines. Moreover, their electroanalytical determination in pharmaceutical formulations, urine and blood plasma samples is discussed. The need for rapid, easy and low-cost detection and quantification of these compounds in complex samples led to the development of sensors based on modified electrodes with nanostructured materials, such as carbon nanotubes, carbon nanofibers, graphene related materials, gold nanomaterials, metal nanoparticles, polymers and nanocomposites. The recent electrochemical methodologies and DNA-electrochemical biosensors, developed to study the interaction of alkylating agents with single- and double-stranded DNA molecules, are presented. These studies are essential for the development of improved antineoplastic drugs, enabling to obtain real-time information concerning the mechanism of action of the alkylating agents and how they mediate the oxidative DNA damage. The DNA electrochemical biosensors allow the in situ real-time determination of the DNA interaction mechanisms with the alkylating agents, with their degradation products, with their redox reaction products, or with their metabolites.

CRediT authorship contribution statement

Ana-Maria Chiorcea-Paquim: Conceptualization, Methodology, Writing – original draft, Writing – review & editing. **Ana Maria Oliveira Brett:** Conceptualization, Resources, Writing – review & editing.

Declaration of Competing Interest

The authors declare that they have no known competing financial interests or personal relationships that could have appeared to influence the work reported in this paper.

Data availability

Data will be made available on request.

Acknowledgments

This research was sponsored by FEDER funds through the program COMPETE–Programa Operacional Factores de Competitividade, and by national funds through FCT–Fundação para a Ciência e a Tecnologia, under the project UID/EMS/00285/2020.

References

[1] S. Puyo, D. Montaudon, P. Pourquier, From old alkylating agents to new minor groove binders, Crit. Rev. Oncol. Hematol. 89 (2014) 43–61, https://doi.org/10.1016/j.critrevonc.2013.07.006.
[2] R. Thirumaran, G.C. Prendergast, P.B. Gilman, Cytotoxic chemotherapy in clinical treatment of cancer, Cancer Immunotherapy, 2007, pp. 101–116. ⟨DOI: 10.1016/B978-012372551-6/50071-7⟩.
[3] D. Fu, J.A. Calvo, L.D. Samson, Balancing repair and tolerance of DNA damage caused by alkylating agents, Nat. Rev. Cancer 12 (2012) 104–120, https://doi.org/10.1038/nrc3185.
[4] L. Sreerama, Alkylating Agents, Encycl, in: M. Schwab (Ed.), Cancer, Springer Berlin Heidelberg, Berlin, Heidelberg, 2011, pp. 132–136, https://doi.org/10.1007/978-3-642-16483-5_182.
[5] F. Lehmann, J. Wennerberg, Evolution of nitrogen-based alkylating anticancer agents, Processes 9 (2021) 1–10, https://doi.org/10.3390/pr9020377.
[6] M. Ghalkhani, I.P.G. Fernandes, S.C.B. Oliveira, S. Shahrokhian, A.M. Oliveira-Brett, Electrochemical redox behaviour of temozolomide using a glassy carbon electrode, Electroanalysis 22 (2010) 2633–2640, https://doi.org/10.1002/elan.201000272.
[7] I.C. Lopes, S.C.B. De Oliveira, A.M. Oliveira-Brett, Temozolomide chemical degradation to 5-aminoimidazole-4-carboxamide - electrochemical study, J. Electroanal. Chem. 704 (2013) 183–189, https://doi.org/10.1016/j.jelechem.2013.07.011.
[8] P.K. Pathak, A. Kumar, B.B. Prasad, A novel electrocatalytic nanocomposite of reduced graphene oxide/silver nanocube hybrid decorated imprinted polymer for ultra-trace sensing of temozolomide, New J. Chem. 42 (2018) 13486–13496, https://doi.org/10.1039/c8nj01824c.
[9] J.R.B. Rodriguez, A.C. Garcia, A.J.M. Ordieres, P.T. Blanco, Electrochemical oxidation of dacarbazine and its major metabolite (AIC) on carbon electrodes, Electroanalysis 1 (1989) 529–534, https://doi.org/10.1002/elan.1140010609.
[10] A.J.M. Ordieres, A.C. Garcia, P.T. Blanco, W.F. Smyth, An electroanalytical study of the anticancer drug dacarbazine, Anal. Chim. Acta 202 (1987) 141–149, https://doi.org/10.1016/S0003-2670(00)85909-7.
[11] Y.M. Temerk, M.M. Kamal, M.S. Ibrahim, H. Ibrahim, W. Schuhmann, Electrochemical behaviour of the anticancer dacarbazine-Cu2+ complex and its analytical applications, Electroanalysis 23 (2011) 1638–1644, https://doi.org/10.1002/elan.201100038.
[12] S. Deepa, B.E.K. Swamy, K.V. Pai, A surfactant SDS modified carbon paste electrode as an enhanced and effective electrochemical sensor for the determination of doxorubicin and dacarbazine its applications: a voltammetric study, J. Electroanal. Chem. 879 (2020), https://doi.org/10.1016/j.jelechem.2020.114748.
[13] S. Dehdashtian, N. Behbahanian, K.M. Taherzadeh, An ultrasensitive electrochemical sensor for direct determination of anticancer drug dacarbazine based on multiwall carbon nanotube-modified carbon paste electrode and application in pharmaceutical sample, J. Iran. Chem. Soc. 15 (2018) 931–941, https://doi.org/10.1007/s13738-018-1291-5.
[14] M. Ibrahim, Y. Temerk, H. Ibrahim, Fabrication of a new biosensor based on a Sn doped ceria nanoparticle modified glassy carbon paste electrode for the selective determination of the anticancer drug dacarbazine in pharmaceuticals, RSC Adv. 7 (2017) 32357–32366, https://doi.org/10.1039/c7ra04331g.
[15] M. Satyanarayana, K. Yugender Goud, K. Koteshwara Reddy, K. Vengatajalabathy Gobi, Conducting polymer-layered carbon nanotube as sensor interface for electrochemical detection of dacarbazine in-vitro, Electrocatalysis 8 (2017) 214–223, https://doi.org/10.1007/s12678-017-0357-y.
[16] B.B. Prasad, P.K. Pathak, Development of surface imprinted nanospheres using the inverse suspension polymerization method for electrochemical ultra sensing of dacarbazine, Anal. Chim. Acta 974 (2017) 75–86, https://doi.org/10.1016/j.aca.2017.04.001.
[17] S.C.B. Oliveira, C.H.S. Mendes, F.F.S. Filho, N.L. Queiroz, J.A.M. Nascimento, V. B. Nascimento, Electrochemical oxidation mechanism of procarbazine at glassy carbon electrode, J. Electroanal. Chem. 746 (2015) 51–56, https://doi.org/10.1016/j.jelechem.2015.02.033.
[18] V.V. Tkach, S.C de Oliveira, S.K.B. de Oliveira, R. Ogani, O V. Elenich, P. I. Yagodynets, The mechanism for the electrooxidation of procarbazine pharmaceutical preparation in alkaline media and its mathematical description, Chim. Techno Acta 3 (2016) 85–95, https://doi.org/10.15826/chimtech.2016.3.1.007.
[19] V.V. Tkach, S.C.B. de Oliveira, S.C.B. de Oliveira, V.S. Neves, R. Ojani, P. I. Yagodynets, The electrochemical oxidation of procarbazine on Cobalt(III) oxyhydroxide and its mathematical evaluation, Anal. Bioanal. Electrochem. 8 (2016) 432–441.
[20] J.P. McCue, J.H. Kennedy, Oxidation of procarbazine in the presence of Ti(IV, Bioinorg. Chem. 7 (1977) 5–21, https://doi.org/10.1016/S0006-3061(00)80125-8.

[21] M. Seenu Naik, M. Siva Prasad, I. Chenna Reddy, N.Y. Sreedhar, Voltammetric determination of streptozotocin in pharmaceutical and human urine samples using glassy carbon electrode modified with polyaniline based nanosensors, Int. J. Pharm. Ther. 6 (2015) 59–63.
[22] C.N. Reddy, P. Reddyprasad, N. Sreedhar, Electrochemical analysis of antichemotherapeutic drug zanosar in pharmaceutical and biological samples by differential pulse polarography, J. Anal. Methods Chem. 2013 (2013), https://doi.org/10.1155/2013/420761.
[23] C. Cojocel, L. Novotny, A. Vachalkova, B. Knauf, Comparison of the carcinogenic potential of streptozotocin by polarography and alkaline elution, Neoplasma 50 (2003) 110–116.
[24] S. Keraghel, O. Dehbi, F. Benghanem, Electrochemical behaviour and differential pulse cathodic adsorptive stripping voltammetric determination of carmustine, Chem. Sci. Trans. (2018), https://doi.org/10.7598/cst2018.1489.
[25] K. Pecková, L. Vrzalová, V. Bencko, J. Barek, Voltammetric and amperometric determination of n-nitroso antineoplastic drugs at mercury and amalgam electrodes, Collect. Czechoslov. Chem. Commun. 74 (2009) 1697–1713, https://doi.org/10.1135/cccc2009112.
[26] O. Josypčuk, J. Barek, B. Josypčuk, Application of non-stop-flow differential pulse voltammetry at a tubular detector of silver solid amalgam for electrochemical determination of lomustine (CCNU, Electroanalysis 26 (2014) 306–311, https://doi.org/10.1002/elan.201300456.
[27] Y. Temerk, M. Ibrahim, H. Ibrahim, M. Kotb, Adsorptive stripping voltammetric determination of anticancer drug lomustine in biological fluids using in situ mercury film coated graphite pencil electrode, J. Electroanal. Chem. 760 (2016) 135–142, https://doi.org/10.1016/j.jelechem.2015.11.026.
[28] N.A. Alarfaj, M.F. El-Tohamy, Ultrasensitve modified carbon paste inclusion β -cyclodextrin and carbon nanotubes sensors for electrochemical detection of anticancer nimustine hydrochloride, Int. J. Electrochem. Sci. 11 (2016).
[29] A. Erol, F. Akpınar, M. Muti, Electrochemical determination of anticancer drug Bendamustine and its interaction with double strand DNA in the absence and presence of quercetin, Colloids Surf. B Biointerfaces 205 (2021), https://doi.org/10.1016/j.colsurfb.2021.111884.
[30] H. Setiyanto, V. Saraswaty, R. Hertadi, I. Noviandri, B. Buchari, Cyclic voltammetric study of chlorambucil in the presence of 4-chloro butyronitrile in aqueous solution, Int. J. ChemTech Res. 3 (2011) 1986–1992.
[31] K. Sakthivel, A. Muthumariappan, S.M. Chen, Y.L. Li, T.W. Chen, M.A. Ali, Evaluating ternary metal oxide (TMO)core-shell nanocomposites for the rapid determination of the anti-neoplastic drug Chlorambucil (Leukeran™) by electrochemical approaches, Mater. Sci. Eng. C 103 (2019), 109724, https://doi.org/10.1016/j.msec.2019.05.009.
[32] B.B. Prasad, R. Singh, A. Kumar, Synthesis of fullerene (C60-monoadduct)-based water-compatible imprinted micelles for electrochemical determination of chlorambucil, Biosens. Bioelectron. 94 (2017) 115–123, https://doi.org/10.1016/j.bios.2017.02.040.
[33] B. Mutharani, P. Ranganathan, S.M. Chen, H.C. Tsai, Temperature-responsive voltammetric sensor based on stimuli-sensitive semi-interpenetrating polymer network conductive microgels for reversible switch detection of nitrogen mustard analog chlorambucil (Leukeran™), Electrochim. Acta 374 (2021), https://doi.org/10.1016/j.electacta.2021.137866.
[34] J. Barek, A. Berka, J. Zima, Determination of melphalanusing differential pulse voltammetry, Anal. Lett. 18 (1985) 2581–2589, https://doi.org/10.1080/00032718508064488.
[35] J. Barek, J. Matějka, J. Zima, Polarographic and voltammetric determination of chlorobenzene, benzyl chloride and melphalan, Collect. Czechoslov. Chem. Commun. 57 (1992) 450–456, https://doi.org/10.1135/cccc19920450.
[36] P. Sinha, S. Doi, D.K. Sharma, Electrochemical behaviour and adsorptive stripping voltammetric determination of cyclophosphamide, Chem. Sci. Trans. (2018), https://doi.org/10.7598/cst2018.1414.
[37] B. Huang, L. Xiao, H. Dong, X. Zhang, W. Gan, S. Mahboob, et al., Electrochemical sensing platform based on molecularly imprinted polymer decorated N,S co-doped activated graphene for ultrasensitive and selective determination of cyclophosphamide, Talanta 164 (2017) 601–607, https://doi.org/10.1016/j.talanta.2016.11.009.
[38] S.S. Hassan, M.M. Amer, S.A. Abd El-Fatah, A.M. El-Kosasy, Microcoated wire sensors for the determination of anticancer drugs cyclophosphamide and ifosphamide in the presence of their degradates, Talanta 46 (1998) 1395–1403, https://doi.org/10.1016/S0039-9140(98)00008-3.
[39] B. Hatamluyi, F. Lorestani, Z. Es'haghi, Au/Pd@rGO nanocomposite decorated with poly (L-Cysteine) as a probe for simultaneous sensitive electrochemical determination of anticancer drugs, Ifosfamide and Etoposide, Biosens. Bioelectron. 120 (2018) 22–29, https://doi.org/10.1016/j.bios.2018.08.008.
[40] P.K. Kalambate, A. Dhanjai, Y. Sinha, Y. Li, Y. Shen, Huang, An electrochemical sensor for ifosfamide, acetaminophen, domperidone, and sumatriptan based on self-assembled MXene/MWCNT/chitosan nanocomposite thin film, Microchim. Acta 187 (2020), https://doi.org/10.1007/s00604-020-04366-9.
[41] B. Bali Prasad, A. Kumar, R. Singh, Synthesis of novel monomeric graphene quantum dots and corresponding nanocomposite with molecularly imprinted polymer for electrochemical detection of an anticancerous ifosfamide drug, Biosens. Bioelectron. 94 (2017) 1–9, https://doi.org/10.1016/j.bios.2017.02.028.
[42] D. Marín, R. Valera, E. De La Red, C. Teijeiro, Electrochemical study of antineoplastic drug thiotepa hydrolysis to thiol form and thiotepa-DNA interactions, Bioelectrochem. Bioenerg. 44 (1997), https://doi.org/10.1016/S0302-4598(97)00044-5.
[43] P. Zuman, P. Pérez, D. Marín, Preliminary contribution to the complex reduction processes involving mitomycin C, Electroanalysis 12 (2000) 952–959, https://doi.org/10.1002/1521-4109(200008)12:12<952::AID-ELAN952>3.0.CO;2-J.
[44] G.M. Rao, A. Begleiter, J.W. Lown, J.A. Plambeck, Electrochemical studies of antitumor antibiotics: II. polarographic and cyclic voltammetric studies of mitomycin C, J. Electrochem. Soc. 124 (1977) 199–202, https://doi.org/10.1149/1.2133265.
[45] P. Pérez, C. Teijeiro, D. Marín, Study on the adsorption properties of the drug mitomycin C by stripping voltammetry, Langmuir 18 (2002) 1760–1763, https://doi.org/10.1021/la011213k.
[46] C. Teijeiro, P. Perez, D. Marín, E. Paleček, Cyclic voltammetry of mitomycin C and DNA, Bioelectrochem. Bioenerg. 38 (1995) 77–83, https://doi.org/10.1016/0302-4598(95)01791-C.
[47] Ş. Özalp-Yaman, A.M. Önal, L. Türker, Electrochemical and quantum chemical studies on mitomycin and adriamycin, J. Mol. Struct. 654 (2003) 81–93, https://doi.org/10.1016/S0022-2860(03)00176-5.
[48] M. Tomasz, R. Lipman, M.S. Lee, G.L. Verdine, K. Nakanishi, Reaction of acid-activated mitomycin C with calf thymus DNA and model guanines: elucidation of the base-catalyzed degradation of N7-alkylguanine nucleosides, Biochemistry 26 (1987) 2010–2027, https://doi.org/10.1021/bi00381a034.
[49] E.E.S. Bruzaca, I.C. Lopes, E.H.C. Silva, P.A.V. Carvalho, A.A. Tanaka, Electrochemical oxidation of the antitumor antibiotic mitomycin C and in situ evaluation of its interaction with DNA using a DNA-electrochemical biosensor, Microchem. J. 133 (2017) 81–89, https://doi.org/10.1016/j.microc.2017.03.030.
[50] M. Mehmandoust, F. Uzcan, M. Soylak, N. Erk, Dual-response electrochemical electrode for sensitive monitoring of topotecan and mitomycin as anticancer drugs in real samples, Chemosphere 291 (2022), https://doi.org/10.1016/j.chemosphere.2021.132809.
[51] A.-M. Chiorcea-Paquim, P.V. Santos, R. Eritja, A.M. Oliveira-Brett, Self-assembled G-quadruplex nanostructures: AFM and voltammetric characterization, Phys. Chem. Chem. Phys. 15 (2013) 9117–9124, https://doi.org/10.1039/c3cp50866h.
[52] A.-M. Chiorcea-Paquim, A.D.R. Pontinha, A.M. Oliveira-Brett, Time-dependent polyguanylic acid structural modifications, Electrochem. Commun. 45 (2014) 71–74, https://doi.org/10.1016/j.elecom.2014.05.019.
[53] A.M. Oliveira-Brett, V.C. Diculescu, T.A. Enache, I.P.G. Fernandes, A.M. Chiorcea-Paquim, S.C.B. Oliveira, Bioelectrochemistry for sensing amino acids, peptides, proteins and DNA interactions, Curr. Opin. Electrochem. 14 (2019) 173–179, https://doi.org/10.1016/j.coelec.2019.03.008.
[54] A.M. Chiorcea-Paquim, A.M. Oliveira-Brett, Nanostructured material–based electrochemical sensing of oxidative DNA damage biomarkers 8-oxoguanine and 8-oxodeoxyguanosine: a comprehensive review, Microchim. Acta 188 (2021), https://doi.org/10.1007/s00604-020-04689-7.
[55] A.M. Chiorcea-Paquim, A.M. Oliveira-Brett, DNA electrochemical biosensors for in situ probing of pharmaceutical drug oxidative dna damage, Sensors 21 (2021) 1–26, https://doi.org/10.3390/s21041125.
[56] A.M. Chiorcea-Paquim, 8-oxoguanine and 8-oxodeoxyguanosine biomarkers of oxidative dna damage: a review on HPLC–ECD determination, Molecules 27 (2022), https://doi.org/10.3390/molecules27051620.
[57] J. Labuda, A.M. Oliveira Brett, G. Evtugyn, M. Fojta, M. Mascini, M. Ozsoz, et al., Electrochemical nucleic acid-based biosensors: concepts, terms, and methodology (IUPAC technical report), Pure Appl. Chem. 82 (2010) 1161–1187, https://doi.org/10.1351/PAC-REP-09-08-16.
[58] A.M. Oliveira-Brett, A.M.C. Paquim, V.C. Diculescu, J.A.P. Piedade, Electrochemistry of nanoscale DNA surface films on carbon, 963–70, Med. Eng. Phys. 28 (2006), https://doi.org/10.1016/j.medengphy.2006.05.009.
[59] A.M. Oliveira Brett, V.C. Diculescu, A.M. Chiorcea-Paquim, S.H.P. Serrano, Electrochemical Sensor Analysis, Elsevier, 2007, pp. 413–437. ⟨DOI: 10.1016/S0166-526X(06)49020-6⟩.
[60] A.M. Oliveira Brett, V.C. Diculescu, A.-M. Chiorcea Paquim, S.H.P. Serrano, A.M. Chiorcea-Paquim, S.H.P. Serrano, Chapter 20 DNA-electrochemical biosensors for investigating DNA damage, Comprehensive Analytical Chemistry, Elsevier, 2007, pp. 413–437. ⟨DOI: 10.1016/S0166-526X(06)49020-6⟩.
[61] V.C. Diculescu, A.-M. Chiorcea Paquim, A.M. Oliveira Brett, Electrochemical DNA sensors for detection of DNA damage, Sensors 5 (2005) 377–393.
[62] V.C. Diculescu, A.-M. Chiorcea-Paquim, A.M. Oliveira-Brett, Applications of a DNA-electrochemical biosensor, TrAC Trends Anal. Chem. 79 (2016) 23–36, https://doi.org/10.1016/j.trac.2016.01.019.
[63] S.C.B. De Oliveira, V.C. Diculescu, A.M. Chiorcea Paquim, A.M. Oliveira-Brett, Electrochemical biosensors for DNA-drug interactions, in: Encyclopedia of Interfacial Chemistry: Surface Science and Electrochemistry, Elsevier, 2018, pp. 124–139, https://doi.org/10.1016/B978-0-12-409547-2.13499-7.
[64] A.-M. Chiorcea-Paquim, S.C. Oliveira, V.C. Diculescu, A.M. Oliveira-Brett, Applications of DNA-electrochemical biosensors in cancer research, in: D. Barcelo, P.-D. Hansen, I. Palchetti (Eds.), Comprehensive Analytical Chemistry, Elsevier, 2017, pp. 287–336, https://doi.org/10.1016/bs.coac.2017.06.003.
[65] S.C.B. Oliveira, A.M. Chiorcea-Paquim, S.M. Ribeiro, A.T.P. Melo, M. Vivan, A. M. Oliveira-Brett, In situ electrochemical and AFM study of thalidomide–DNA interaction, Bioelectrochemistry 76 (2009) 201–207, https://doi.org/10.1016/j.bioelechem.2009.03.003.
[66] O. Corduneanu, A.-M. Chiorcea-Paquim, V. Diculescu, S.M. Fiuza, M.P. M. Marques, A.M. Oliveira-Brett, DNA interaction with palladium chelates of biogenic polyamines using atomic force microscopy and voltammetric characterization, Anal. Chem. 82 (2010) 1245–1252, https://doi.org/10.1021/ac902127d.

[67] A.D.R. Pontinha, S.M.A. Jorge, A.M. Chiorcea Paquim, V.C. Diculescu, A. M. Oliveira-Brett, In situ evaluation of anticancer drug methotrexate-DNA interaction using a DNA-electrochemical biosensor and AFM characterization, Phys. Chem. Chem. Phys. 13 (2011) 5227–5234, https://doi.org/10.1039/c0cp02377a.
[68] A.-M. Chiorcea-Paquim, A.D.R. Pontinha, R. Eritja, G. Lucarelli, S. Sparapani, S. Neidle, et al., Atomic force microscopy and voltammetric investigation of quadruplex formation between a triazole-acridine conjugate and guanine-containing repeat DNA sequences, 6141–9, Anal. Chem. 87 (2015), https://doi.org/10.1021/acs.analchem.5b00743.
[69] V.C. Diculescu, A.-M. Chiorcea-Paquim, R. Eritja, A.M. Oliveira-Brett, Evaluation of the structure–activity relationship of thrombin with thrombin binding aptamers by voltammetry and atomic force microscopy, J. Electroanal. Chem. 656 (2011) 159–166, https://doi.org/10.1016/j.jelechem.2010.11.037.
[70] A.-M. Chiorcea-Paquim, O. Corduneanu, S.C.B. Oliveira, V.C. Diculescu, A. M. Oliveira-Brett, Electrochemical and AFM evaluation of hazard compounds–DNA interaction, Electrochim. Acta 54 (2009) 1978–1985, https://doi.org/10.1016/j.electacta.2008.07.032.
[71] T.A. Enache, A.-M. Chiorcea-Paquim, O. Fatibello-Filho, A.M. Oliveira-Brett, Hydroxyl radicals electrochemically generated in situ on a boron-doped diamond electrode, Electrochem. Commun. 11 (2009) 1342–1345, https://doi.org/10.1016/j.elecom.2009.04.017.
[72] S.C.B. Oliveira, A.M. Oliveira-Brett, Boron doped diamond electrode pre-treatments effect on the electrochemical oxidation of dsDNA, DNA bases, nucleotides, homopolynucleotides and biomarker 8-oxoguanine, J. Electroanal. Chem. 648 (2010) 60–66, https://doi.org/10.1016/j.jelechem.2010.06.020.
[73] S.C.B. Oliveira, A.M. Oliveira-Brett, In situ DNA Oxidative damage by electrochemically generated hydroxyl free radicals on a boron-doped diamond electrode, Langmuir 28 (2012) 4896–4901, https://doi.org/10.1021/la300070x.
[74] J.A.P. Piedade, P.S.C. Oliveira, M.C. Lopes, A.M. Oliveira-Brett, Voltammetric determination of γ radiation-induced DNA damage, Anal. Biochem. 355 (2006) 39–49, https://doi.org/10.1016/j.ab.2006.05.022.
[75] H.R.S. Lima, J.S. da Silva, E.A. de Oliveira Farias, P.R.S. Teixeira, C. Eiras, L.C. C. Nunes, Electrochemical sensors and biosensors for the analysis of antineoplastic drugs, Biosens. Bioelectron. 108 (2018) 27–37, https://doi.org/10.1016/j.bios.2018.02.034.
[76] A.M. Oliveira-Brett, J.A.P. Piedade, L.A. Silva, V.C. Diculescu, Voltammetric determination of all DNA nucleotides, Anal. Biochem. 332 (2004) 321–329, https://doi.org/10.1016/j.ab.2004.06.021.
[77] A.M. Oliveira Brett, Electrochemical DNA assays, in: P.N. Bartlett (Ed.), Bioelectrochemistry: Fundamentals, Experimental Techniques and Application, John Wiley & Sons, Ltd, Chichester, UK, 2008, p. 411. ⟨DOI: 10.1002/9780470753842⟩.
[78] I.C. Lopes, S.C.B. Oliveira, A.M. Oliveira-Brett, In situ electrochemical evaluation of anticancer drug temozolomide and its metabolites-DNA interaction, Anal. Bioanal. Chem. 405 (2013) 3783–3790, https://doi.org/10.1007/s00216-012-6546-x.
[79] C. Altay, E. Eksin, G. Congur, A. Erdem, Electrochemical monitoring of the interaction between Temozolamide and nucleic acids by using disposable pencil graphite electrodes, Talanta 144 (2015) 809–815, https://doi.org/10.1016/j.talanta.2015.07.017.
[80] S.N. Topkaya, G. Serindere, M. Ozder, Determination of DNA hypermethylation using anti-cancer drug-temozolomide, Electroanalysis 28 (2016) 1052–1059, https://doi.org/10.1002/elan.201501027.
[81] S. Jahandari, M.A. Taher, H. Karimi-Maleh, A. Khodadadi, E. Faghih-Mirzaei, A powerful DNA-based voltammetric biosensor modified with Au nanoparticles, for the determination of Temodal; an electrochemical and docking investigation, J. Electroanal. Chem. 840 (2019) 313–318, https://doi.org/10.1016/j.jelechem.2019.03.049.
[82] A.E. Radi, A. Eissa, H.M. Nassef, Voltammetric and spectroscopic studies on the binding of the antitumor drug dacarbazine with DNA, J. Electroanal. Chem. 717–718 (2014) 24–28, https://doi.org/10.1016/j.jelechem.2014.01.007.
[83] E. Eksin, D. Polat, A. Erdem, Voltammetric and impedimetric detection of interaction between dacarbazine and nucleic acids, Electroanalysis 31 (2019) 2012–2019, https://doi.org/10.1002/elan.201900284.
[84] E. Kanat, E. Eksin, B. Karacicek, Y. Eraç, A. Erdem, Electrochemical detection of interaction between dacarbazine and nucleic acids in comparison to agarose gel electrophoresis, Electroanalysis 30 (2018) 1566–1574, https://doi.org/10.1002/elan.201800064.
[85] Y. Temerk, H. Ibrahim, Binding mode and thermodynamic studies on the interaction of the anticancer drug dacarbazine and dacarbazine-Cu(II) complex with single and double stranded DNA, J. Pharm. Biomed. Anal. 95 (2014) 26–33, https://doi.org/10.1016/j.jpba.2014.02.010.
[86] M. Song, R. Zhang, X. Wang, Nano-titanium dioxide enhanced biosensing of the interaction of dacarbazine with DNA and DNA bases, Mater. Lett. 60 (2006) 2143–2147, https://doi.org/10.1016/j.matlet.2005.12.100.
[87] Q. Shen, X. Wang, D. Fu, The amplification effect of functionalized gold nanoparticles on the binding of anticancer drug dacarbazine to DNA and DNA bases, Appl. Surf. Sci. 255 (2008) 577–580, https://doi.org/10.1016/j.apsusc.2008.06.132.
[88] R. Zhang, X. Wang, S. Gong, A voltammetric study of the effect of gold nanoparticles on the binding of DTIC to DNA bases, Electrochem. Solid-State Lett. 7 (2004), https://doi.org/10.1149/1.1758933.
[89] R.Y. Zhang, X.M. Wang, S.J. Gong, N.Y. He, Electrochemical detection of single A-G mismatch using biosensing surface based on gold nanoparticles, Genom. Proteom. Bioinform. 3 (2005) 47–51, https://doi.org/10.1016/S1672-0229(05)03007-X.
[90] P.A.V. Carvalho, I. Campelo Lopes, E.H.C. Silva, E.E.S. Bruzaca, H.J. Alves, M.I. S. Lima, et al., Electrochemical behaviour of anticancer drug lomustine and in situ evaluation of its interaction with DNA, J. Pharm. Biomed. Anal. 176 (2019), https://doi.org/10.1016/j.jpba.2019.112786.
[91] Y. Temerk, M. Ibrahim, H. Ibrahim, M. Kotb, Interactions of an anticancer drug lomustine with single and double stranded DNA at physiological conditions analyzed by electrochemical and spectroscopic methods, J. Electroanal. Chem. 769 (2016) 62–71, https://doi.org/10.1016/j.jelechem.2016.03.020.
[92] H. Mahmoudi-Moghaddam, Z. Garkani-Nejad, A new electrochemical DNA biosensor for determination of anti-cancer drug chlorambucil based on a polypyrrole/flower-like platinum/NiCo2O4/pencil graphite electrode, RSC Adv. 12 (2022) 5001–5011, https://doi.org/10.1039/d1ra08291d.
[93] P. Palaska, E. Aritzoglou, S. Girousi, Sensitive detection of cyclophosphamide using DNA-modified carbon paste, pencil graphite and hanging mercury drop electrodes, Talanta 72 (2007) 1199–1206, https://doi.org/10.1016/j.talanta.2007.01.013.
[94] S. Wang, R. Wang, P. Sellin, S. Chang, Carbon nanotube based DNA biosensor for rapid detection of anti-cancer drug of cyclophosphamide, Curr. Nanosci. 5 (2009) 312–317, https://doi.org/10.2174/157341309788921372.
[95] A.E. Radi, H.M. Nassef, A. Eissa, Electrochemical study of the interaction of the alkylating agent busulfan with double strand DNA, Electroanalysis 25 (2013) 2463–2469, https://doi.org/10.1002/elan.201300294.
[96] P. Perez, C. Teijeiro, D. Marin, Interactions of surface-confined DNA with electroreduced mitomycin C comparison with acid-activated mitomycin C, Chem. Biol. Interact. 117 (1999) 65–81, https://doi.org/10.1016/S0009-2797(98)00098-2.
[97] E. Eksin, H. Karadeniz, A. Erdem, Voltammetric and impidimetric detection of anticancer drug mitomycin C and DNA interaction by using carbon nanotubes modified electrodes, Curr. Bionanotechnol. 1 (2015) 32–36, https://doi.org/10.2174/2213529401666150218194827.
[98] D. Ozkan, H. Karadeniz, A. Erdem, M. Mascini, M. Ozsoz, Electrochemical genosensor for Mitomycin C-DNA interaction based on guanine signal, J. Pharm. Biomed. Anal. 35 (2004) 905–912, https://doi.org/10.1016/j.jpba.2004.03.001.
[99] A.A. Ensafi, M. Amini, B. Rezaei, Impedimetric DNA-biosensor for the study of anti-cancer action of mitomycin C: comparison between acid and electroreductive activation, Biosens. Bioelectron. 59 (2014) 282–288, https://doi.org/10.1016/j.bios.2014.03.041.
[100] A. Erdem, M. Muti, P. Papakonstantinou, E. Canavar, H. Karadeniz, G. Congur, et al., Graphene oxide integrated sensor for electrochemical monitoring of mitomycin C-DNA interaction, Analyst 137 (2012) 2129–2135, https://doi.org/10.1039/c2an16011k.
[101] C. Sengiz, G. Congur, E. Eksin, A. Erdem, Multiwalled carbon nanotubes-chitosan modified single-use biosensors for electrochemical monitoring of drug-DNA interactions, Electroanalysis 27 (2015) 1855–1863, https://doi.org/10.1002/elan.201500107.
[102] E. Eksin, M. Muti, A. Erdem, Chitosan/ionic liquid composite electrode for electrochemical monitoring of the surface-confined interaction between mitomycin C and DNA, Electroanalysis 25 (2013) 2321–2329, https://doi.org/10.1002/elan.201300188.
[103] M. Findik, H. Bingol, A. Erdem, Hybrid nanoflowers modified pencil graphite electrodes developed for electrochemical monitoring of interaction between Mitomycin C and DNA, Talanta 222 (2021), 121647, https://doi.org/10.1016/j.talanta.2020.121647.
[104] F. Kuralay, Y. Bayramlı, Electrochemical determination of Mitomycin C and Its interaction with double-stranded DNA Using a poly(o-phenylenediamine)-multi-walled carbon nanotube modified pencil graphite electrode, Anal. Lett. 54 (2021) 1295–1308, https://doi.org/10.1080/00032719.2020.1801710.
[105] E. Canavar, F. Kuralay, A. Erdem, Interaction of mitomycin C with DNA immobilized onto single-walled carbon nanotube/polymer modified pencil graphite electrode, Electroanalysis 23 (2011) 2343–2349, https://doi.org/10.1002/elan.201100149.
[106] H. Karadeniz, L. Alparslan, A. Erdem, E. Karasulu, Electrochemical investigation of interaction between mitomycin C and DNA in a novel drug-delivery system, J. Pharm. Biomed. Anal. 45 (2007) 322–326, https://doi.org/10.1016/j.jpba.2007.05.005.